

# Chapter1 Introduction

## 1.1 General

In the world of the beginning 21st century life has become more energy demanding than ever before. New technology achievements that make our life easier are continuously being introduced and become available to more and more people. This development is reflected in an increased demand of electrical energy. A key invention that allowed and drives this development is the gas turbine power plane. This machine converts chemical energy of fuel into kinetic energy. The operating principle of gas turbines is described by the Brayton cycle thermodynamic model. The machine consists of three main components, compressor, combustor and turbine. Air is first compressed from a low to a high pressure, at which it is used to burn fuel in a combustor, to add energy into the cycle. In the turbine section the combusted fuel/air mixture is expanded from high pressure and temperature back to the low pressure level. The turbine expansion process partly converts the energy of the mixture in kinetic energy, which is used to drive the compressor and additional pay loads. Nowadays, gas turbines are mostly used in power plants to generate electrical power, or for creating thrust in jet engines of airplanes. In all fields of applications gas turbines work in highly competitive markets. Therefore, they are judged by their efficiency, power density, manufacturing and operating costs and emissions [4].

The turbine section is composed of stationary and rotating blade rows, called turbine stages. A stator row deflects and accelerates the working medium in circumferential direction. A rotor row positioned directly downstream of the stator converts the kinetic energy of the fluid into angular momentum by turning the fluid back in to the axial direction. The expansion process in the turbine blade a number of loss creating mechanisms. In order to increase the efficiency, and reduces fuel consumption and increases the economic operation of these machine. Therefore study the detailed and fundamental comprehension of loss mechanisms is necessary.

In general application of turbomachinery, the aerodynamic losses are generated from a number of sources. [1] States that, losses are typically broken down into profile loss, end wall loss, and tip leakage loss. Profile loss is loss generated in the blade boundary layers and blade wakes. End wall loss refers to loss that is a result of the end wall boundary layer passing through the tip clearance. Tip leakage loss pertains to losses incurred by the flow that passes through the blade tip clearance from pressure side to suction side. The leakage flow through the clearance causes both end wall loss and leakage loss. [2] Stated that the most important loss generation mechanisms are.

1. The blade-tip-end wall clearance flow.
2. The interaction of blade and end wall boundary layers with the flow in the Blade tip region, and.
3. The diffusion and mixing of flows.

The loss of flow through the tip clearance from the main passage and the subsequent irreversible mixing and diffusion that are the sources of inefficiency. From the list of loss generation mechanisms, the first two items create three distinct vortices: the tip leakage vortex, the horseshoe vortex, and the passage (or cross flow) vortex. Figure 1.1 and figure 1.2 shows these near-tip flow phenomena that are traditionally found to occur in a turbomachine. In some cases, the tip leakage flow may roll-up and form a discrete vortex. In a typical turbine figure 1.1 show, the tip leakage flow could be found in turbine, compressor and fan flow fields. Figure 1.2(a) shows a qualitative drawing of the tip leakage vortex that is created by the flow that leaks through the tip clearance. Figure 1.2(b) illustrates the stagnation point, or horseshoe vortex, as well as the passage vortex on one side of the blade. In Figure 1.2(c), a different view of the passage vortex is given [2].

Understanding and analyzing of the effects of tip clearance on axial turbine performance is very important to increase the turbomachinery performance (high

efficiency, reduce losses, low noise, ect) and to make any improvement of turbomachinery design so as to reduce the losses of flow through the tip clearance in turbomachines. The present study focus to study effect one of the losses occur in turbine on the rotor performance. Losses are created by the fluid that passes through the radial gap between the tips of the rotor blades and the stationary casing. A rotor row in turbine has a small distance between the tip of the rotor blade and casing is called a tip clearance. It is necessary for the rotor to be able to move, this gap allow the working fluid to leak through the gap from pressure side to suction side, the tip leakage flow is driven by the pressure difference between the pressure side and suction side of the blade.

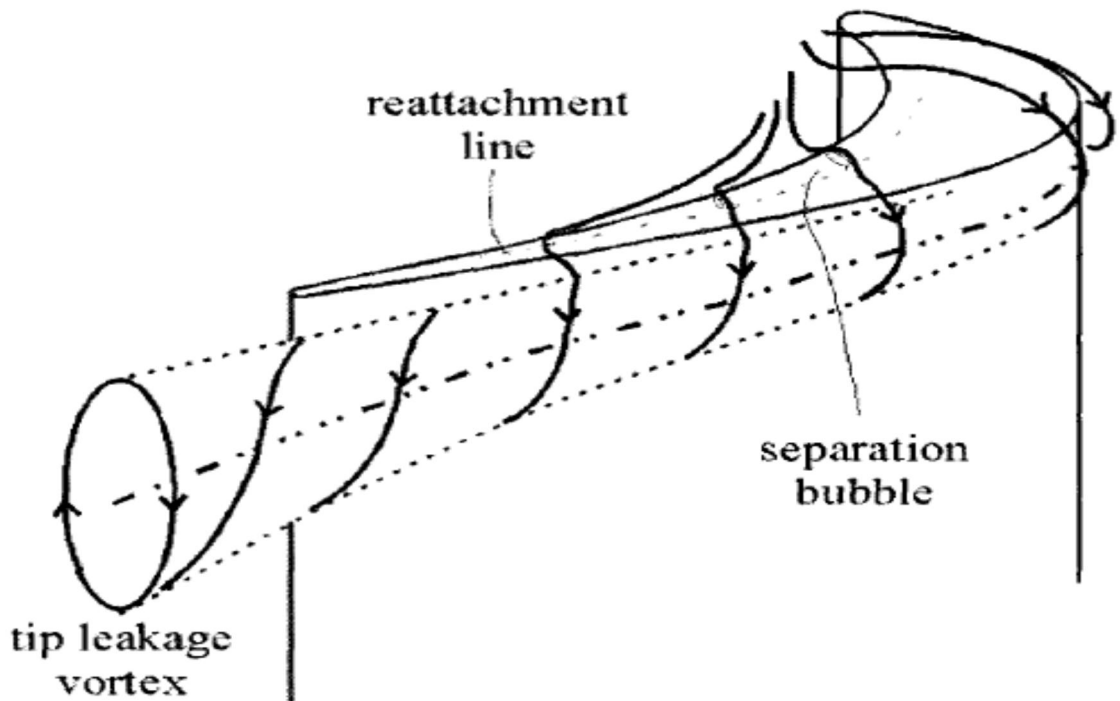
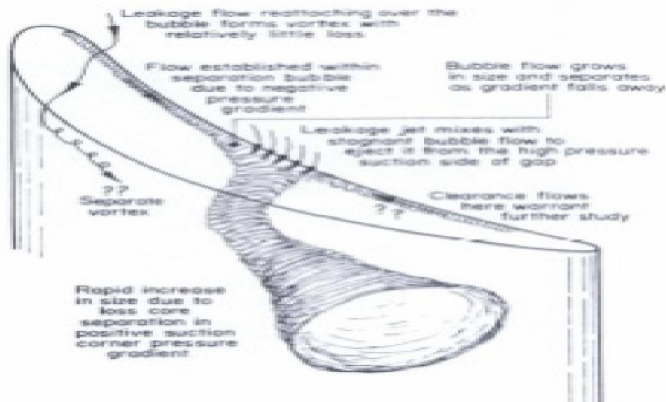
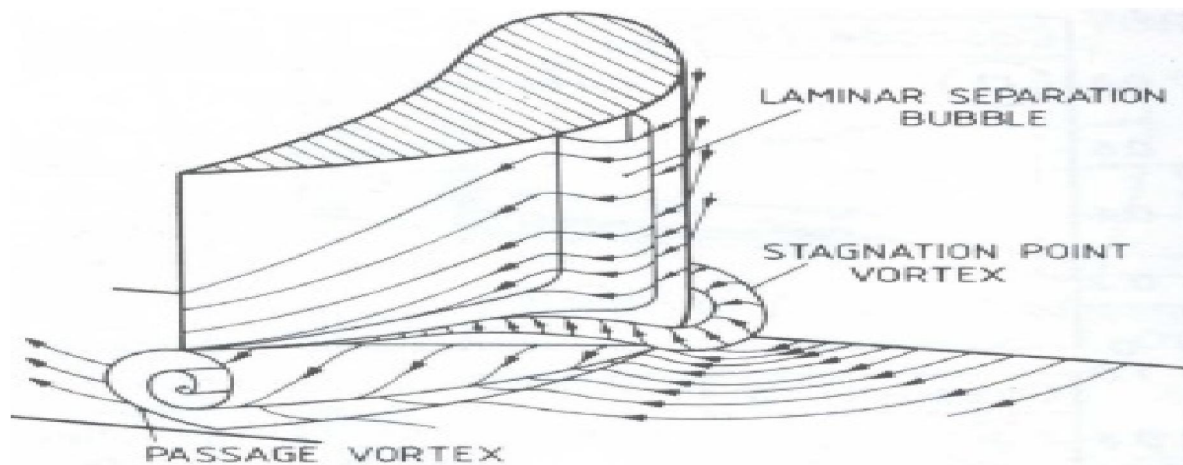


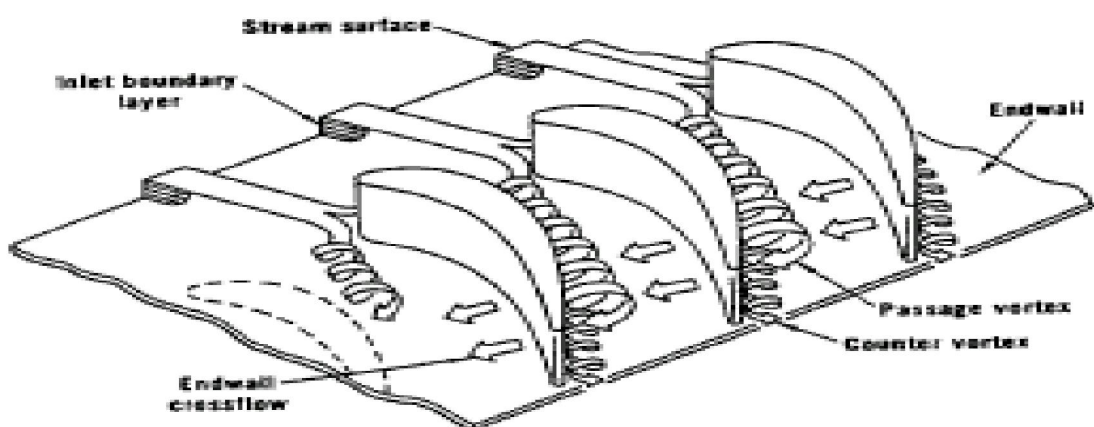
Figure1.1. Schematic of a typical turbine tip leakage vortex[32]



(a)



(b)



(c)

Fig.1.2. Near-tip Coherent Vortex Structures

(a) Tip Leakage Vortex; taken from Bindon, [31], (b) Horseshoe and Passage Vortices; taken from Lakshminarayana, ,(c) Passage Vortex; taken from Lakshminarayana,[2]

## **1.2-Objective**

The objective of the present research aims to use numerical simulation to Study the behavior of flow inside axial flow rotor for the purpose to analyze and understand the phenomena of tip leakage flow which occur inside it, and to study the effect of this phenomena, on the performance of the axial flow rotor, and determine their directions, their dominant regions, and their resulting vortex, at different tip clearance, and different rotating speeds.

## **1.3-Scope of the thesis**

The present research presented in the following ways. First, general introduction in Chapter 1. Second literature review of the earlier studies, selected from the relevant field, will be presented in Chapter 2. Following these, numerical approach along with the details CFD software will be given in chapter 3. Result and discussion In Chapter 4, Finally, conclusions, and future directions that are required for further study of the effect of tip clearance on rotor Performance.

# Chapter2 Literature review

## 2.1 Introduction.

In order to improve the performance of turbomachinery systems, a detailed understanding of the complex and highly three-dimensional flow phenomena inside axial flow turbine is required. Tip leakage flows one of this phenomena are very complicated by their interaction with the passage flow and the boundary layer developed from the end wall. With the rapid progress of computer and CFD technologies in recent years, many researchers have a tendency to use numerical investigation to solve this problem. But currently, the turbulence structure generated by this phenomenon is not well understood and remains difficult to predict. Experimental study still plays an important role in the study of tip leakage flows. It can give us detailed views of the fundamentals of such flow phenomena, and can also provide valuable data to establish and modify the models used in numerical investigation. Accordingly the focus of this chapter is to frame the present work by reviewing different numerical simulations.

## 1.3. Losses in Turbomachines

Losses in turbomachines are historically classified by their origin and thus termed as, profile loss, end wall loss, tip clearance loss.

### 1.3.1 Profile Loss

This loss is associated with the growth of the boundary layer which is directly related to blade profile. When the adverse pressure gradient on the surfaces so this increase profile losses by the separation of boundary layer. The pattern of the boundary layer growth and its separation depend on the geometries of the blade and flow. The suction side of a blade is more prone to boundary layer separation than pressure side of blade. So the suction side aerodynamic losses higher than pressure side of blade surfaces U.J.Patdiwala et al [4].

### 1.3.2 End wall Losses

This loss occurs in the regions of flow near the end walls owing to the presence of unwanted circulatory or cross flows. The flow near the end wall give rise to circulatory flows which are mixes with main flow through the blade passage. As a result of this, secondary vortices in the stream wise direction are generated in the blade passages. These vortices try to transport low energy fluid from the pressure side to suction side of the blade passage, thus increasing the possibility of separation of the boundary layer on the suction side. Figure.2.1 show end wall losses Flow structure in a turbine cascade [1].

### 1.2.3 Tip Clearance Flow Losses

These losses arise due to the clearance between a moving blade and the cas. On account of the static pressure difference, the flow leaks from the pressure side towards to suction side. Figure2.2 show CFD tip leakage flow.

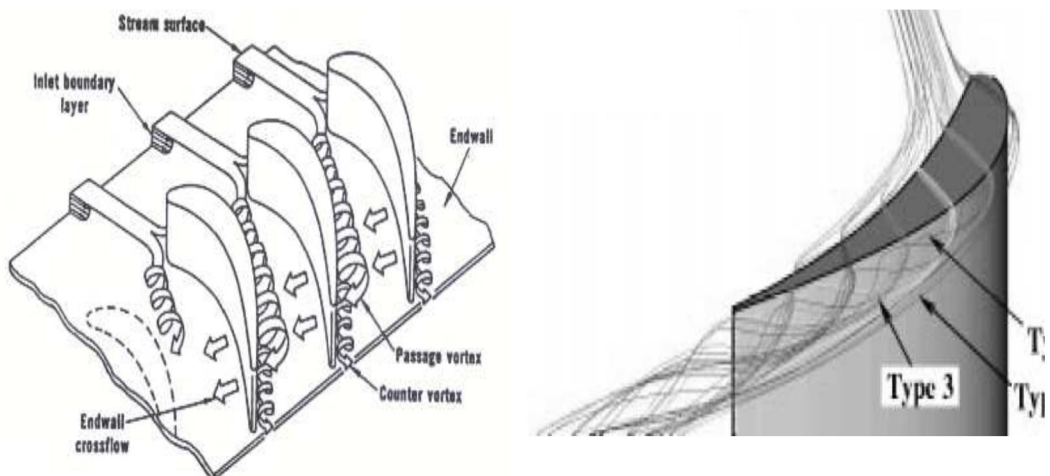


Figure2.1.Behavior of secondary flows as proposed by Langston[5]

Figure 2.2 Tip-gap flows from a numerical model by Tallman and Lakshminara-Yana [6]

### 3-Tip leakage flow studies

The tip leakage flows are one of the most common and influential features of flow through turbomachines. In fact tip leakage flows are important source of unsteadiness and three dimensionality of flow in turbomachines, while contributing significantly to loss of efficiency and useful work in turbomachines.

#### 3.1 Formation of tip leakage flow

Fundamentally, a leakage flow can be decomposed into two driving components: one which results from the static pressure gradient between the pressure side and suction side of the blade, and a second which is driven by the relative motion of the adjacent rotating casing. The first driving component, pressure gradient, occurs as a result of the airfoil shape of the blade, thereby creating a high-pressure PS and a low-pressure SS. The clearance between the blade tip and the casing, allows space for pressure-driven flow to escape around the blade tip Figure.2.3 show that. The second driving component, the moving wall, forms as a derivation of the Couette flow problem. In this case, viscous stresses create a shear flow which is additive to the pressure-driven flow, Adams, N.G., and Hepworth, H.K, [7].

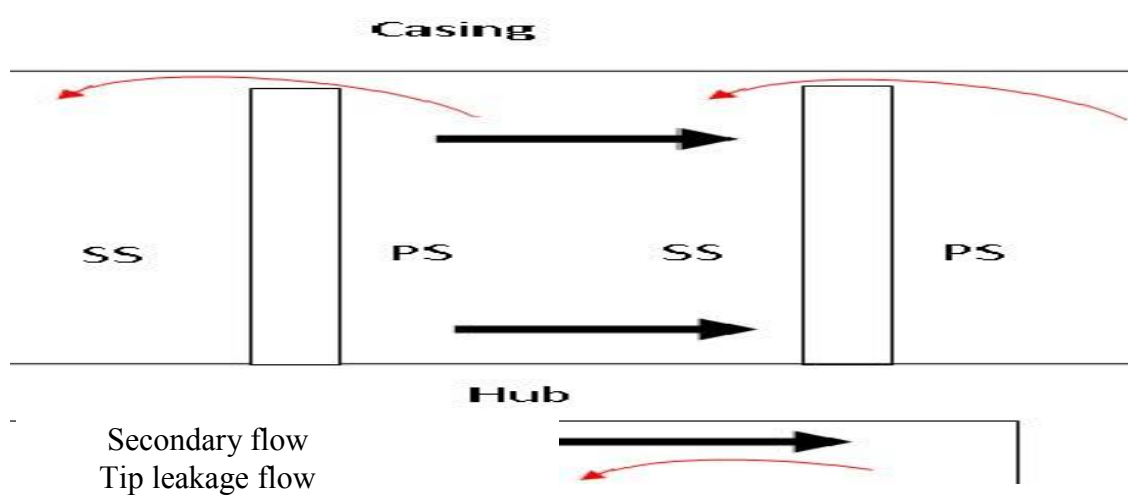


Fig.2.3 representation of pressure-driven flow from blade PS to blade SS [5 ].

The effects of turbine tip clearance on gas turbine performance studied by Cleverson Bringhenti and Joao Roberto Barbosa [8]. They observed that the tip clearance have very well affect on its performance and occurs losses. They also found that the turbine tip clearance effect also seen by the compressor characteristics and the engine performance. And this information used during early design phase to take into account of turbine tip clearance losses. Anderson Jr [9] evaluation of tip-leakage flows based on tip-clearance variations using a computational fluid dynamics (CFD) to predict the variations in pressure ratio, efficiency and mass flow for different gap clearances. Krishnababu et al.[10] published a numerical study to evaluate influence of different tip geometries on the tip leakage flow and heat transfer, based on flat tip geometry and squealer type geometries, comparing two different tip clearance gaps. It was observed that, in comparison with the simple geometries, the squealer type geometries are advantageous aerodynamically and for heat transfer, because they decrease leakage flow, and hence losses and average heat transfer at the tip.

Muthanna [11] builted an 8 blades, 7 passage linear compressor cascade with tip leakage. He measured the flow field downstream of the cascade using four sensor hot-wire anemometers, from which he obtained the mean velocity field, the turbulence stress field and velocity spectra. He used oil flow visualizations on the end wall underneath the blade row. He studied the effects of tip gap height, and blade boundary layer trip variations. He observed an existence of two distinct vertical structures in the flow. The tip leakage vortex which formed due to the roll up of the tip flow as it exits the tip gap region. A second vortex, counter-rotating when compared to the tip leakage vortex, is formed due to the separation of the flow leaving the tip gap from the end wall. He found that an increase in the tip gap height increases the strength of the tip leakage vortex, and vice versa. He also found that changing the boundary layer trip had no effect on the flow field. RajeshYadav et al [12] Investigations of Gas Turbine Characteristics by Varying Tip Clearance and Axial Gap for different values of axial gap varying from 2.5 mm to 4.5 mm with the interval of 0.5 mm and a tip clearance out of values 3%, 5% and 7%.thy found that the effect of axial and tip clearance that the efficiency is maximum for the combination of 3.5 mm axial gap

and tip clearance 3%. But for the actual case, the tip clearance of 3% is not sufficient because of thermal expansion of rotor blade working under high temperature and rotating with high speed. J.S. Liu and R. Bozzola[13]used Three-Dimensional Navier-Stokes Analysis of the Tip Clearance Flow in Linear Turbine Cascades. Huanxin [14] used Simple-type method based on three-dimensional non-stagger grids in body-fitted coordinate, Navier-Stokes equations closed by  $k-\varepsilon$  turbulence model and Euler equations to simulate and analyze three dimensional flow and tip clearance leakage of an isolated axial compressor rotor. His comparison between the numerical and available experimental results showed that leakage flow is invalid and can be controlled by the difference of reduced pressure between pressure side and the suction side of blade at tip region. Sell et al. [15] presented computational tip aerodynamics results from a linear turbine cascade with an exit Mach number of 0.5. They reported that the computational simulations agree well with their measurements.

Ameri et al. [16] computationally investigated the effect of tip recess on tip heat transfer and efficiency. They found that the numerical prediction of the effect of the casing recess on blade and tip heat transfer and efficiency was reliable.

Wu, k., and, Elhadi, E.[17] Simulation of tip leakage flows and their effects in axial flow fan using computational fluid dynamics at deferent tip clearance (0,2,4) size at three different loading conditions; small flow rate, design flow rate and large flow rate. The CFD code was based on solving Reynolds averaged Navier-Stokes equations coupled with Spalart-Allaras turbulence model. They investigation the Effects of tip clearance size on fan performance at different loading conditions and The structure of flow inside the flow inside tip clearance. He found the increase of tip clearance high influence of performance . Adamczyk [19]stated that the stable operation range of a turbomachine is affected by tip clearance. He wrote “Smith found that increasing the clearance between the tips of rotors and the case of low-speed compressor caused the point of stall inception to move to a higher flow rate”.

## 4. Computational Fluid dynamic (CFD) studies

Computational fluid dynamics (CFD) is predicting what will happen, quantitatively, when fluids flow, often with the complications of simultaneous flow of heat, mass transfer (eg perspiration, dissolution), phase change (eg melting, freezing, boiling), chemical reaction (eg combustion, rusting), mechanical movement (eg of pistons, turbine, fans, rudders), stresses in displacement of immersed or surrounding solids. Computational fluid dynamics (CFD) is one of the branches of fluid mechanics that uses numerical methods and algorithms to solve and analyze problems that involve fluid flows. Computers are used to perform the millions of calculations required to simulate the interaction of fluids and gases with the complex surfaces used in engineering. Today Computational Fluid Dynamics tools are becoming standard in many fields of engineering involving flow of gases and liquids. Numerical simulations are used in the design phase to select between different concepts and it is used in the production phase to analyze performance. Accurate and robust turbomachinery flow prediction and study different phenomena that occurs inside machine remains an objective of most researches in turbomachinery field. Representation of flow in turbomachinery is difficult due to existence of viscous wake, secondary flow, turbulence, leakage flow and interaction of different flows from these phenomena. Certainly turbomachinery internal flow analysis and design have benefited greatly from advancements in computational power and efficiency. As stated by Keith [18], "today, 3-D Euler, quasi-3-D viscous, and 3-D full Navier-Stokes analyses are integral parts of turbomachinery design procedures for all engine manufacturers. As noted by Adamczyk [19], today fan rotors are designed using viscous 3D CFD model,..., etc, using these models the blade geometry is tailored to control shock location, boundary layer growth and end-wall blockage". Denton [2] stated: "computational fluid dynamics (CFD) probably plays a greater part in the aerodynamic design of turbomachinery than it does in any other engineering application". Tallman [20] stated "CFD offers a tool for looking at the flow inside

areas too small for measurements. Real engine parameters i.e. physical geometry, boundary conditions, operating conditions and additional forces could be modified much easier in computational study". Accordingly there are many computational fluid dynamics works available in Turbomachinery literature. F.R. Menter et el [20] they using CFD to Simulation OF Turbo Machinery Flows –Verification, Validation and Modeling-( ANSYS – CFX) they found The challenge to the CFD modeler lies in the proper formulation of models, which offer an optimal compromise between robustness, numerical costs and physical accuracy. The challenge to the design engineer lies in the selection of the best model for the application at hand and to provide an adequate space and time resolution of the flow. Basson and Ro [8] Showed that the flow in the casing region of axial rotor is very complex due to existence of blade and end wall boundary layers. He also stated that losses generated as a results of flow leakage and its interaction with other flow are about 30-50% of total loss of rotor. Khalid et el[21] pointed out that the end wall blockage is approximately proportional to clearance height. Tomita, J.T. and Barbosa, J.R. [22] discuss the influence of the flow turbulence intensity in an axial turbine inlet in its design-point operation. The flow calculations were performed by an in house 3D CFD code based on RANS (Reynolds Average Navier-Stokes). The turbulence effect was performed using the one-equation turbulence model developed by Sparlat and Allmaras. The flow was considered completely turbulent. He also discuss the influence of the tip clearance of rotor blades in internal losses, which affect the operation of an axial turbomachine when the pressure ratio and efficiency are analyzed. Elhadi [23] studied and analyzed the behavior of flow in axial flow fan. He used numerical simulations based on Navier-Stoke equations coupled with  $k-\varepsilon$  Turbulence model with standard wall function. This simulation applied to axial flow fan which consists of nine rotor blades and fifteen stator blades .Moore et al [24] predicted the tip clearance flow in a linear turbine cascade with the three-dimensional incompressible Navier-Stokes code. However the flow in turbomachinery components is usually compressible. They comparisons between the computed results and experimental data included important design features such

as exit total pressure and flow angle, plus the flow properties inside the tip clearance region, such as velocity, angle, and pressure .Suneesh [25]analyzed the flow inside axial compressor with the change in axial spacing between blade rows. He used FLUENT code which based on finite volume method for solving Navier-Stopkes equations coupled with  $k-\epsilon$  turbulence model and standard wall function. He found that the unsteadiness in the blade passages increases with a decrease in axial space between blade rows. Tallman [20] wrote in his Master thesis that, in past the application of 3D Navier-Stokes CFD codes to Compressors and turbines has been aimed at validation using direct comparison with measured data. Only recently have researchers begun to use CFD as a tool for prediction. CFD is logically better suited to the study of the fine details of the tip leakage flow and vortex than experimental measurement. Martin [26] used experimental work and FLUENT software package to study the influence of three dimensional boundary layer flows on the stall behavior and flow loss generation inside turbomachinery. He described different kinds of separated flows which can be treated using computational fluid dynamics.

# **Chapter3 Numerical Simulation Techniques**

## **3.1Introduction.**

Fluid flow is commonly studied using one of three Technique theoretical, experimental and numerically using CFD software. The CFD tools to obtain information about the fluid flow problem and the flow parameter like pressure velocity, temperature, heat transfer, mass transfer, chemical reaction and related phenomena by solving mathematical equations which govern these processes using numerical algorithms. The starting point of any numerical method is the mathematical model which represent partial differential equation and boundary conditions and conservation of matter. momentum and energy must be satisfied throughout the region of interest, the solution of conservation equation is post-processed to extract quantities of interest e.g lift , drag ,torque, heat transfer ,pressure losses , leakage flow .....ect. Now a today modern CFD manages to solve laminar flows with ease and good reliability provided that the discriptionization of space or the grid. As well resolved and the boundary condition are properly specified turbulent flow or the hand is more difficult to simulate since the finer features of the flow always are unsteady and three dimensional render. Turbulent eddies in all possible orientations will appear in turbulent flow .Depending on the choice of method used to model the flow more or less computation power and time will be needed.

## **3.2 Solution strategy in fluent software solver.**

Fluent solvers are best on finite volume discretization process .the domain (fluid region) is discretized into finite set of control volume or cell (mesh) general conservation (transport) equation of mass flow ,momentum and energy are described into algebra equation that can be solved to extract flow field.

### **3.2.1 pre-processing in gambit software**

In per processing step the problem has to be clearly. Used gambit software to create Geometry and Mesh is the first pre-processes the basic steps involve:-

1. Defining the geometry of the region of interest.
2. Creating regions of fluid flow, solid regions and surface boundary names.
3. Setting properties for the mesh.

After the appropriate mesh will be created in pre-processes, the next step choosing the best numerical model in fluent software is allowed to define Physics Definition This interactive process is the second pre- processing stage and is used to create input required by the Solver. The mesh files are loaded into the physics pre-processor. The physical models that are to be included in the simulation are selected. Fluid properties and boundary conditions are specified. the solver and execution once the problem has been pre-processed a numerical model suitable to set up of mathematical nature of problem include the governing equation and turbulent model then the model will be executed and the solution monitored until convergence reaches .

### **3.2.2post-processing in fluent software**

As in the pre-processing huge amount of development work has recently take place in the post processing field. Owing to increased popularity of engineering work stations, many of which has outstanding graphics capabilities, the leading CFD are now equipped with versatile data visualization tools. such as plots, pressure contour ,velocity contours , velocity vector or stream line...ect. the result have to be examined and analyzed the modifications of the model to be considered. In the present study CFD code fluent software will be used for solving executing and post processing.

### 3.3 Governing equation of fluid Dynamic

All fluid flows, whether laminar or turbulent in nature can be described by a set of partial differential equation comprise a set of equation that are conservation law of mass equation momentum and energy equation. The software use in the present work is the commercial software (CFD) code containing the preprocessor, solver and a post-processing tool. CFD codes use the finite volume method (FVM) to discretize the geometry of the flow. This discretization is created upon an integral form of the partial differential equations (conservation of mass, momentum and energy) to be solved. The geometry is divided into cells as small control volumes and the governing equations are solved for each control volume. The numerical simulations in present study steady-state 3D flow field inside the turbine rotor passage with tip clearance are obtained by solving the three dimensional and Navier -Stokes equations coupled with (  $k-\epsilon$  ) turbulent model to algebraic equations that can be solved numerically. A 3D rotor blade passage is used as shown in Figure 3.1.

continuity equation is:

## Conservation of Momentum:

### 3.3 TURBULENCE MODELS

Many turbulence models have been developed in order to solve the RANS governing equations. At the beginning were one equation models (Spalart-Allmaras) and subsequently more effective two-equation models. No one of them, unfortunately, is widely accepted as being superior to others for all cases. The choice of turbulence model depends on considerations such as the geometry of the field, physics in the flow, the level of accuracy required, the available computational resources and the amount of time available for the simulation. Two equation models are considered

nowadays the best way to calculate the unknown variables emerging from the RANS approach. In these models the solution of two separate transport equations allows the turbulent velocity and length scales to be independently determined. Two of the most important of them are the  $k-\epsilon$  model and the  $k-\omega$  model.

### 3.3.2 $k-\epsilon$ turbulence model

The  $K$ -epsilon model is one of the most common turbulence models. It is a tow equation model, that means, it includes two extra transport equations to represent the turbulent properties of the flow. This allows a two equation model to account for history effects like convection and diffusion of turbulent energy. The first transported variable is turbulent kinetic energy,  $k$ . The second transported variable in this case is the turbulent dissipation,  $\epsilon$ . It is the variable that determines the scale of the turbulence, whereas the first variable,  $k$ , determines the energy in the turbulence. There are two major formulations of  $K-\epsilon$  models [28]. That of Launder and **Sharma** [29] is typically called the standard  $k-\epsilon$  Model. The original impetus for the  $k-\epsilon$  model was to improve the mixing-length model, as well as to find an alternative to algebraically prescribing turbulent length scales in moderate to high complexity flows. According to [29], there are three usual  $k-\epsilon$  models:

- Standard  $k-\epsilon$  model.
- RNG  $k-\epsilon$  model.
- Realizable  $k-\epsilon$  model.

The computations in the present study have mainly been carried out using standard  $k-\epsilon$  model, (under the two -equation model category).transport equation is employed in the following form:

turbulent kinetic energy  $k$

$$\left( \frac{\partial}{\partial x_i} (\rho k u_i) \right) = \left( \frac{\partial}{\partial x} \left[ (\mu + \frac{\mu_t}{\sigma_k}) \frac{\partial k}{\partial x_j} \right] + p_k + p_b - \rho \epsilon - Y_M S_k \right) \dots \dots \dots 3.3$$

dissipation  $\epsilon$

$$\left( \frac{\partial}{\partial x_i} (\rho \epsilon u_i) \right) = \left( \frac{\partial}{\partial x_j} \left[ (\mu + \frac{\mu_t}{\sigma_\epsilon}) \frac{\partial \epsilon}{\partial x_j} \right] + C_{1\epsilon} \frac{\epsilon}{k} (P_k + C_{3\epsilon} P_b) - C_{2\epsilon} \rho \frac{\epsilon^2}{k} + S_\epsilon \right) \dots \dots 3.4$$

### 3.4 Model Description

The rotor considered is shown schematically in Figure 3.1. This rotor consists of 60 blade and 400mm diameter for a single stage rotor blade. A steady-state solution for this configuration using only one blade. Computational unstructured mesh is used to mesh the one blade by gambit software. The mesh is hexahedral element grid type. Fig.3.2 shows sample of the mesh at two blades suction side and at region near the hub. The total number of grid is about  $600 \times 10^4$  grid. Static pressure and constant modified turbulence viscosity are set for both inlet and outlet of the rotor. The solver is defined first. Solver is taken as pressure based and formulation as implicit, space as 3D and time as steady. Velocity formulation as absolute and gradient options are taken. The viscous medium is also taken. The analysis is carried using turbulence flow and then the k- $\epsilon$  model is considered. The working material is done is air Present axial flow rotor design conditions shown in table.3.1. The solutions Calculations are carried out for seven different rotation speeds. The solution is said to be convergence for each case when the mass flow rate at the outlet becomes constant.

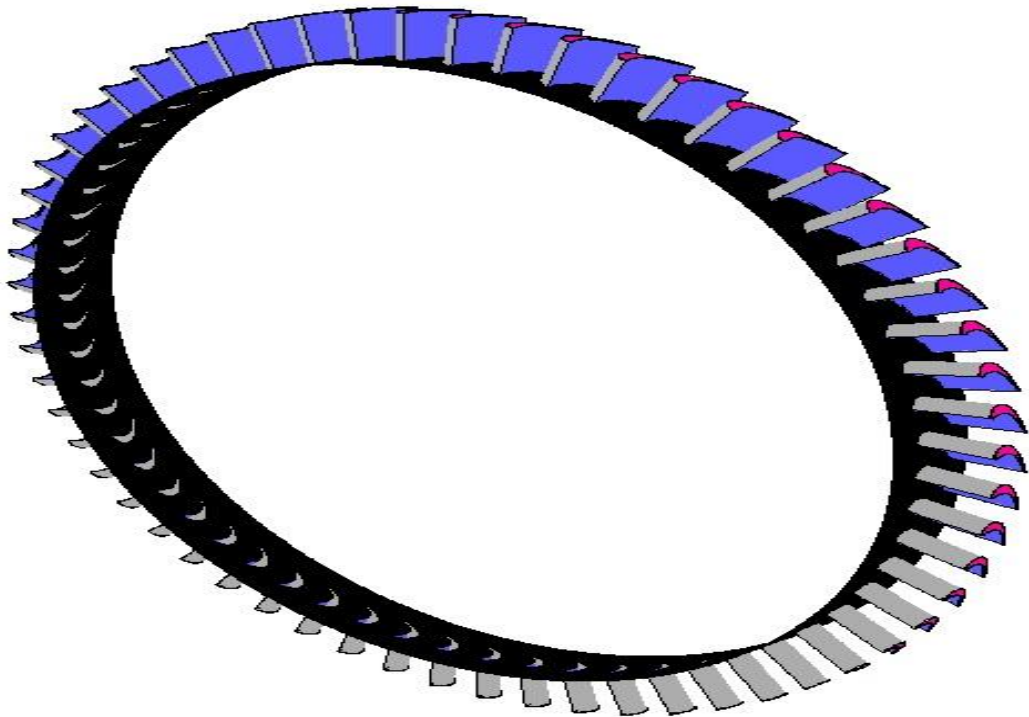


Figure3.1Rotor blade rows

Table 3.1 Present axial flow rotor design conditions.

Casing diameter	400 mm
Rotation speed	3000 RPM
Rotor blade number	60
operating conditions of	101325 Pa
Boundary Conditions	
Inlet Pressure	4.6bar
Outlet Pressure	1.46bar
Inlet Total Temperature	444K
Properties of air	
Cp (specific heat capacity)	1006.43J/kg K
Density	1.125 kg/m <sup>3</sup>
Thermal conductivity	0.0242 W/m K
Viscosity	1.7894e-05 kg/m -s
Fluid Gamma ( $\gamma$ )	1.4

### 3.5 Computational Grid

The computational unstructured mesh used in the present studies are generated for different values of tip clearance gap. The geometry and the computational grid are constructed with fluent software used for preparing input data for CFD programs. The computational grids have about 596863 grid points.

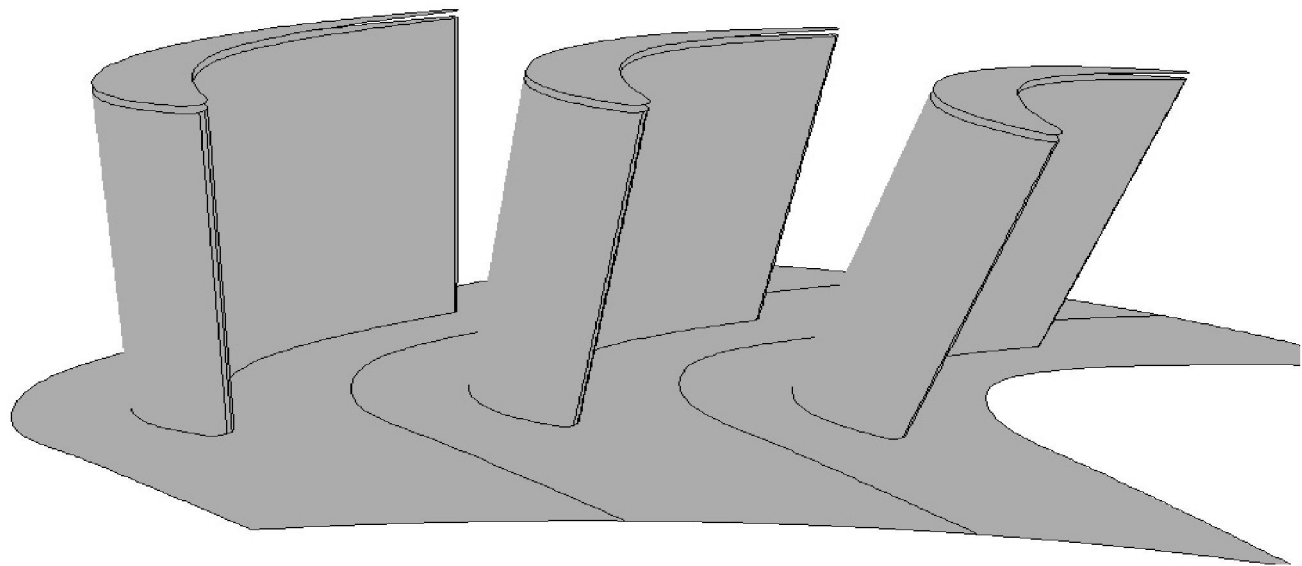


Fig.3.2(a) Computational domain, the view blade wall and hub  
it was tilted for purpose to see it clearly.

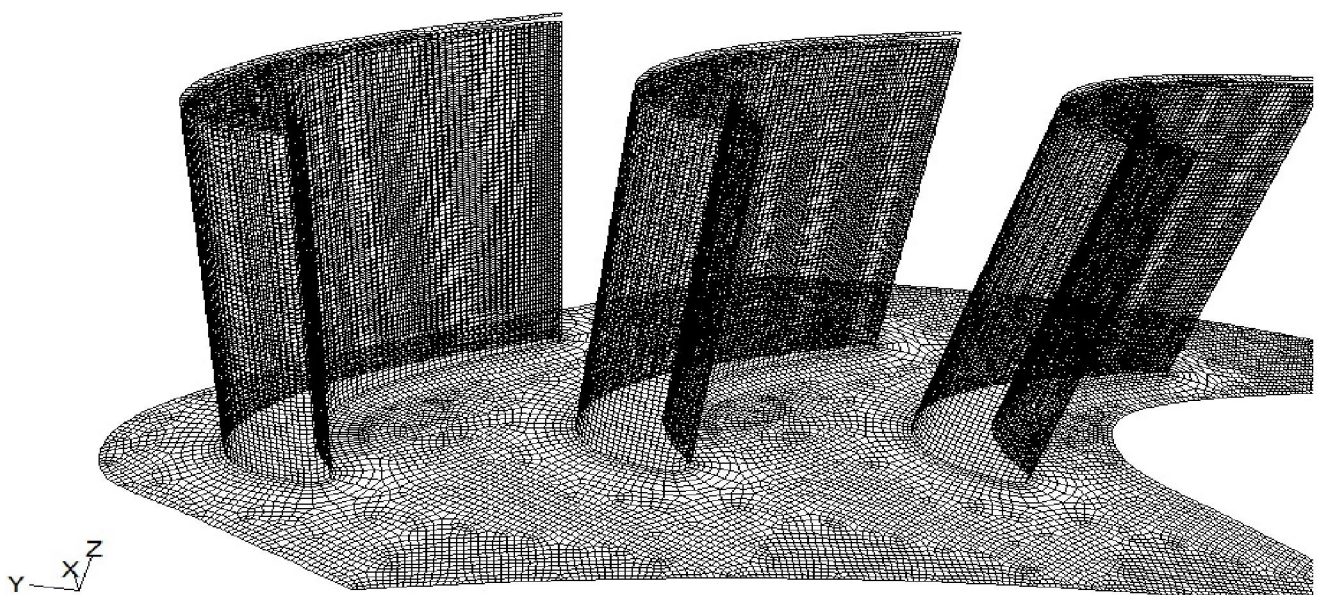


Fig3.3(b) Sample of view for the computational grid

### 3.6 Boundary condition

The common setup for the boundary conditions leading to a stable convergence of the solution is to set the total pressure at the inlet of the model and the static pressure at the outlet. Periodic– Rotational periodic conditions are taken on the two faces of turbo volume .Casing- Casing is considered as stationary wall. Hub–Hub is considered as wall with 0 RPM Relative to Adjacent cell zone. FLUID–Fluid considered here is air and motion type considered is Moving Reference Frame (MRF).The rotational speed is in RPM. PRESSURE SIDE– Pressure side is considered as wall with 0 RPM Relative to Adjacent cell zone. SUCTION SIDE– Suction Side is considered as wall with 0 RPM Relative to Adjacent cell zone.

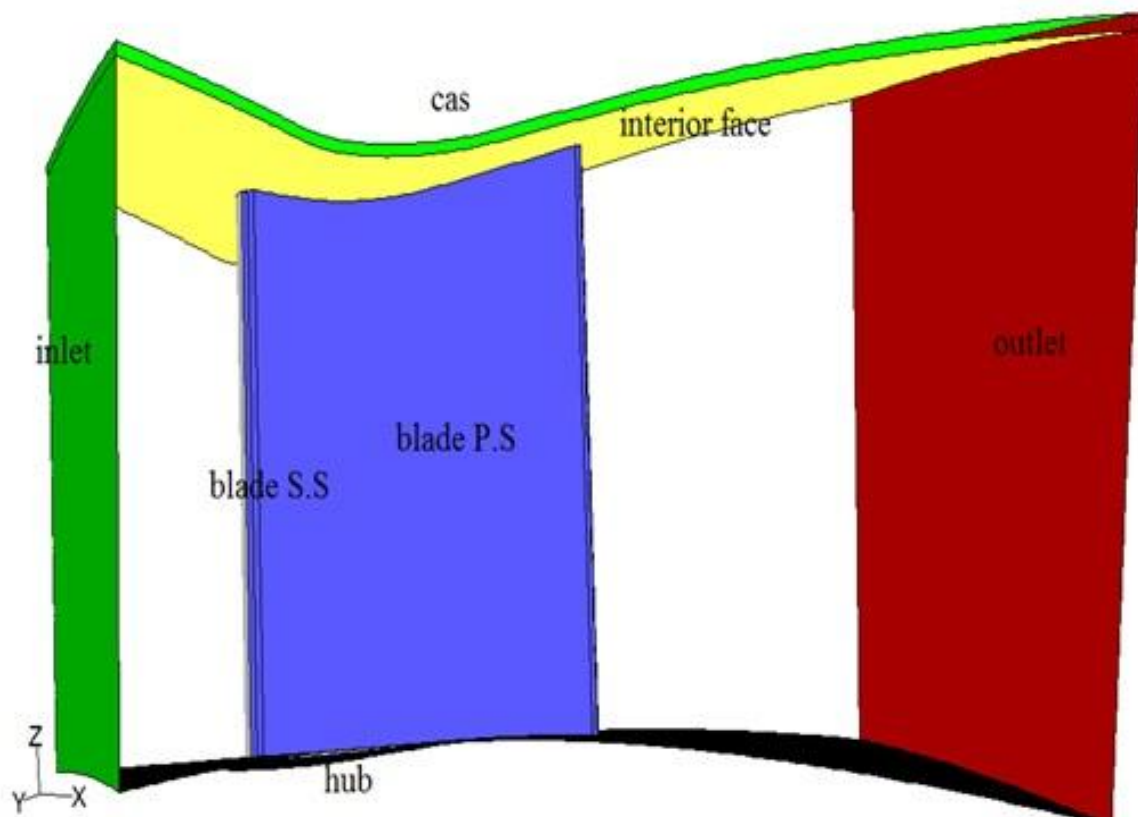


Fig.3.4 Computational domain boundaries

### **3.7 Computational method**

The present simulation used numerical simulation based on a control volume technique to convert the governing equations to algebraic equations that can be solved numerically. The diffusion terms in the govern equations were discretized using power low scheme accurate central difference while the convection terms were discretized using power low scheme. These equations were solved using implicit segerated solver algorithm. This algorithm is based on solving these equations sequentially (i.e., segregated from one another). SIMPLE algorithm method [32] is used for the purpose of coupling between pressure and velocity and satisfying the mass and momentum conservation laws. In order to check the convergence, the mass flow rate at rotor outlet is monitored in each calculation.

### **3.8 Solution control**

The results are obtained with the solution of the continuity, N-S equations along with the equations for the selected turbulence model. In this present study,  $k$ -  $\varepsilon$  model is selected as the turbulence model. After the boundary conditions are specified and the solution models are selected, the iterations are performed in FLUENT Software solver. The required number of iterations is determined by setting convergence criteria for the residuals for the three components of velocities(X,Y,Z), the continuity equation and the variable for the ( $k$  -  $\varepsilon$ ) model.

#### **3.8.1 Convergence criterion**

In most cases, the convergence criterion is set such that the difference between two successive iterations [residuals] is five orders of magnitude lower than the initial value. It is satisfied.

### 3.8.2 Solver Residual

The residual is criteria to measure of the local imbalance of each conservative control volume equation. It is the most important measure of convergence as it relates directly to whether the equations have been solved. The residual is calculated using only the spatial flux terms and essentially represents a discrete conservations balance. The following figure 3.2 show a typical convergence history graph of the solutions. It is seen from the figure that the residuals for the variables are decreased to at least five orders of magnitude and a stable trend is reached at the end.

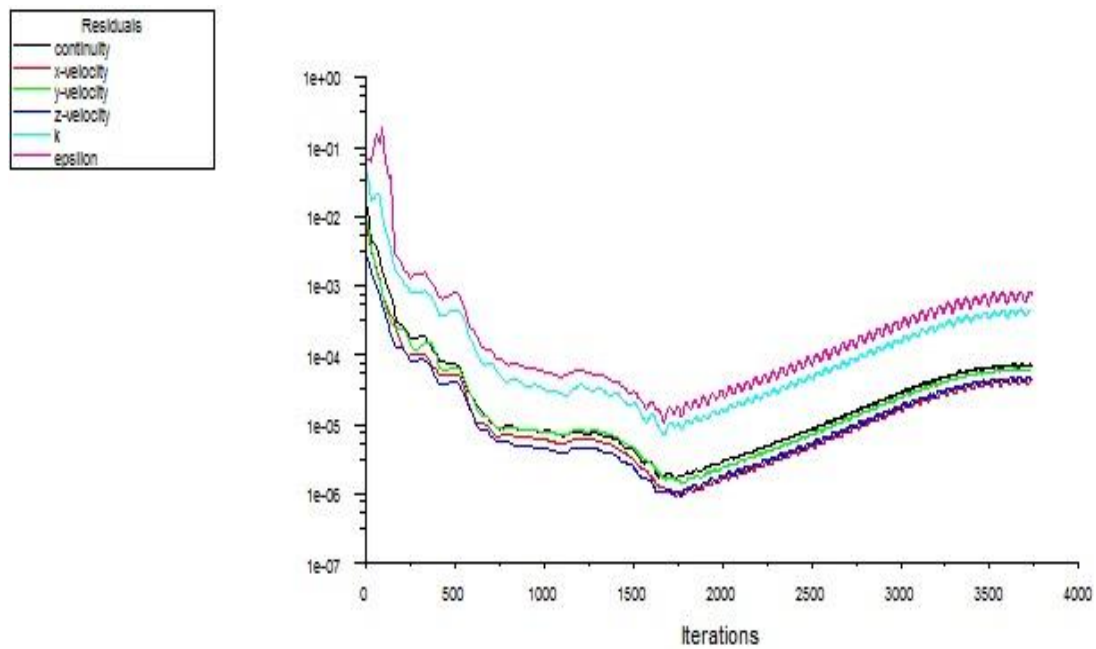


Fig.3.5 a typical convergence residuals.

### 3.5.1.2 Mass flow rate.

A very important information about convergence of the numerical solution is the mass flow rate reaches a constant value between inlet and outlet of the domain. The solution is said to be converged. Mass flow rate of the stationary solutions in the present work is representatively illustrated below in figure (3.6) and is of the order of E-5. Figure 3.6 show Mass Flow rate.

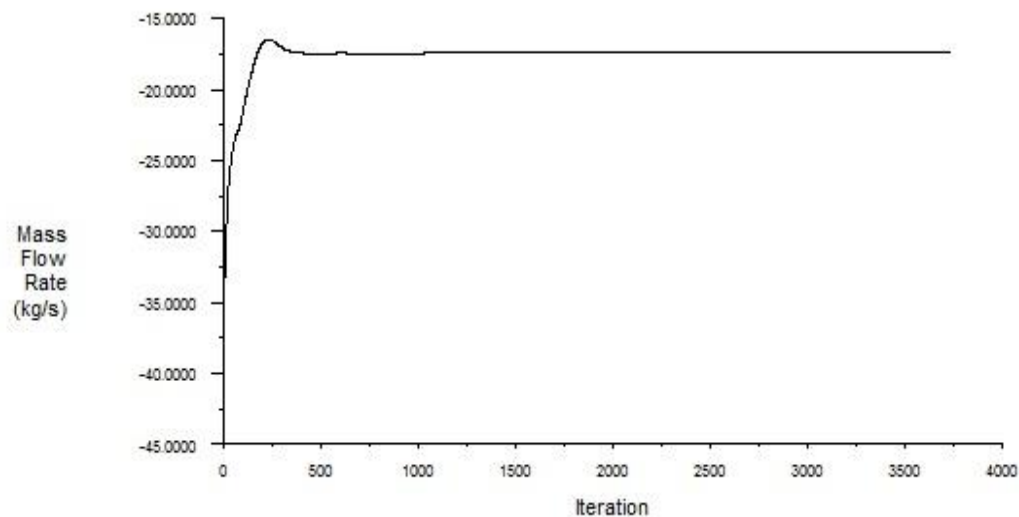


Fig.3.6 show Mass Flow rate of convergence history of mass flow rate on outlet.

## Chapter4 Results and Discussion

### 4.1 Introduction

In order to compare the effect tip clearance size, and rotation speeds on the tip leakage flows structure affected on rotor Performance , calculations were carried out for three cases of tip clearance (0, 4 and 6 mm), and seven different speeds of 1000 rpm , 1500 rpm ,2000rpm ,2500rpm,3000rpm,3500rpm, and 4000rpm were studied.

### 4.2 Effects of Tip clearance size on rotor performance

Table 4.1 and figure4.1 show how the efficiency of rotor ( $\eta$ ) and total pressure (TP) are affected by the tip clearance size at different rotation speeds. The table, and figure show that both efficiency, and total pressure decrease as tip clearance increases. This indicates that tip clearance has a large influence on the performance of rotor. Also figure 4.1 indicates effect of both rotation speed and tip size on turbine performance i.e., an increase in tip clearance from 4mm to 6 mm at 3000rpm results in a 1.6% drop in efficiency, and 2 % reduction in total pressure rise. Also from this figure we can see that maximum efficiency occurs at the tip zero. And increasing of tip clearance, leads to decrease efficiency.

**Table 4.1 Effects of Tip Clearance on rotor Performance**

N (rpm )	$\eta$ / percentage reduction in $\eta$ *			TP(Pa) /percentage reduction in TP *		
	T C(0)	T C (4)	T C (6)	T C (0)	T C (4)	T C (6)
1000	72.064	69.94/2.90	67.77/5.96	614795.56	603148.31/1.9	589867.94/4.05
1500	78.75	75.95/3.56	74.14/5.85	752876.13	737668.2/2.0	725347.88/3.66
2000	81.75	80.70/1.28	78.06/4.52	922058.63	906535/1.68	884617.69/4.06
2500	83.20	80.84/2.84	79.54 /4.49	1121404	1091411.3/2.7	1070019.3 /4.6
3000	83.25	81.14/2.53	79.83/4.10	1355664	1311394.6/3.3	1283913.8 /5.3
3500	83.42	81.13/2.75	80.57/3.42	1614723	1565140/3.1	1448017/ 10.32
4000	81.88	80.65/0.36	79.42/3.00	1873687	1840014/1.8	1790341.8/4.45

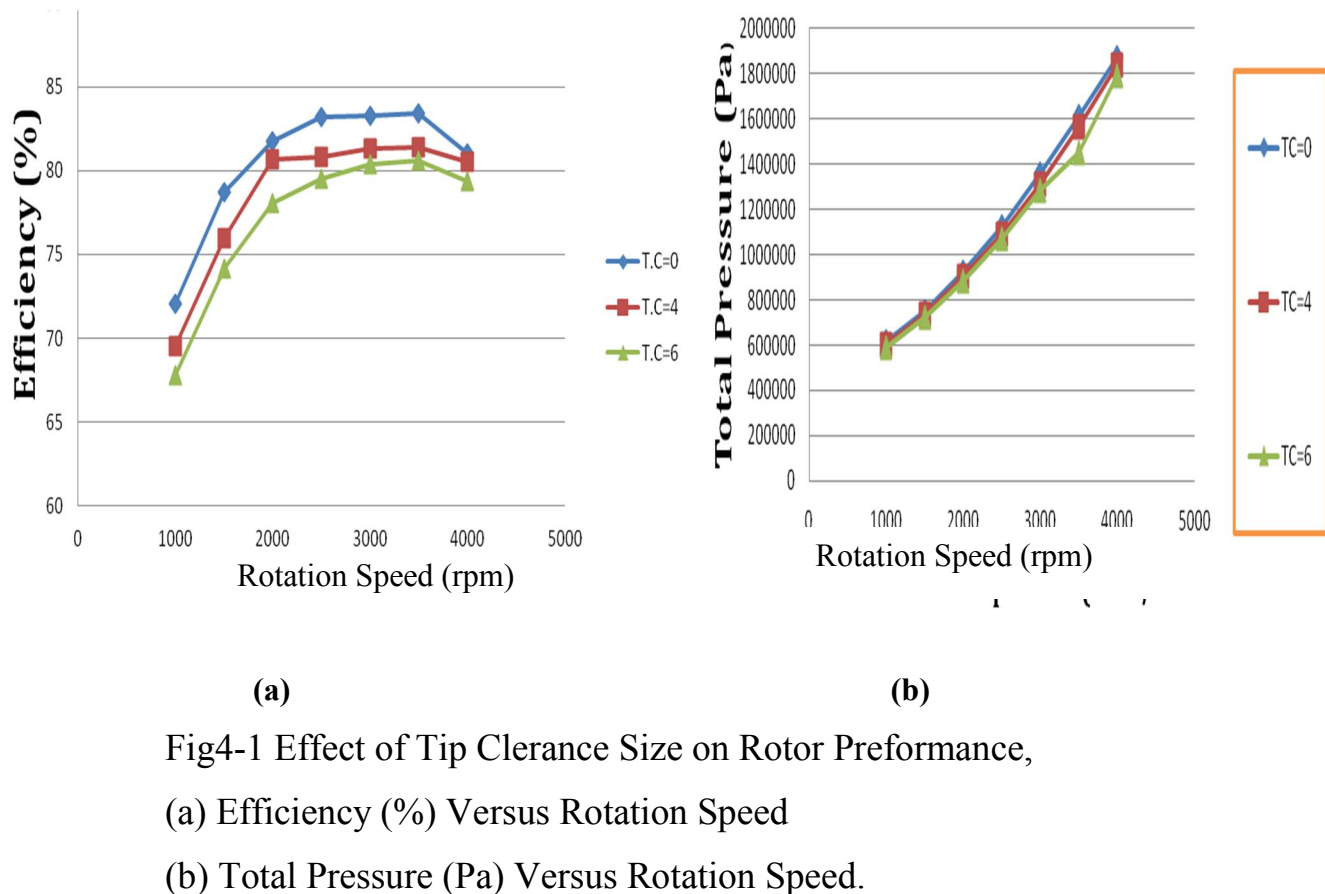
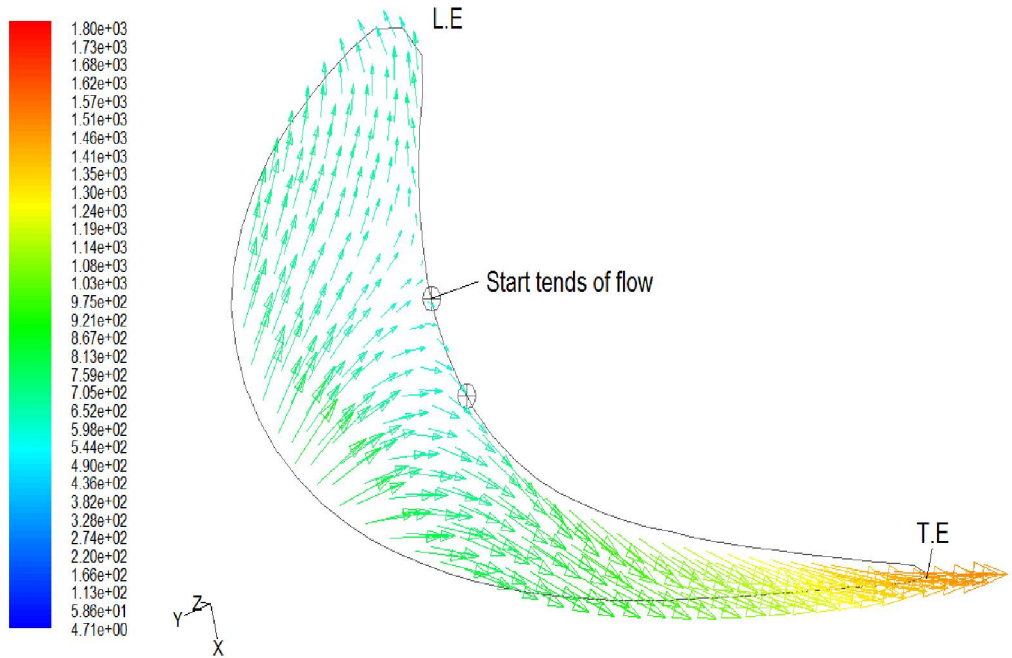


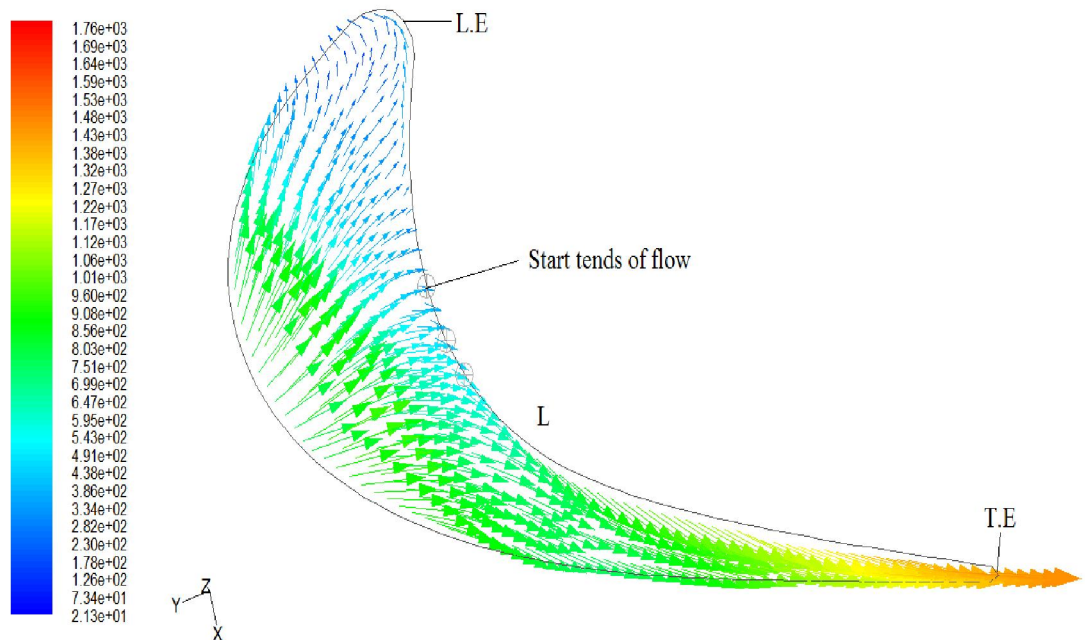
Fig4-1 Effect of Tip Clearance Size on Rotor Performance,  
 (a) Efficiency (%) Versus Rotation Speed  
 (b) Total Pressure (Pa) Versus Rotation Speed.

### **4.3 Flow separation.**

Flow separation is Very important flow phenomena associated with the leakage flow. This phenomenon occurs due to difference in pressure at tip and it obstructs the leakage flow attachment on the tip surface. As shown in Figure. 4.2, the region of the recirculation flow increases with the increase of the tip clearance. This figure indicates that the flow separation starts at 43% of chord from L.E for tip clearance 6mm and about 46.5% of chord from L.E for tip clearance 4mm. It is clearly appear from figure. 4.2 that, the flow separation causes leakage flow from pressure side to suction side through tip clearance. This leakage flow interacts with the overturned end wall flow near the suction surface and rolls down from the end wall to form a leakage vortex.



(a)



(b)

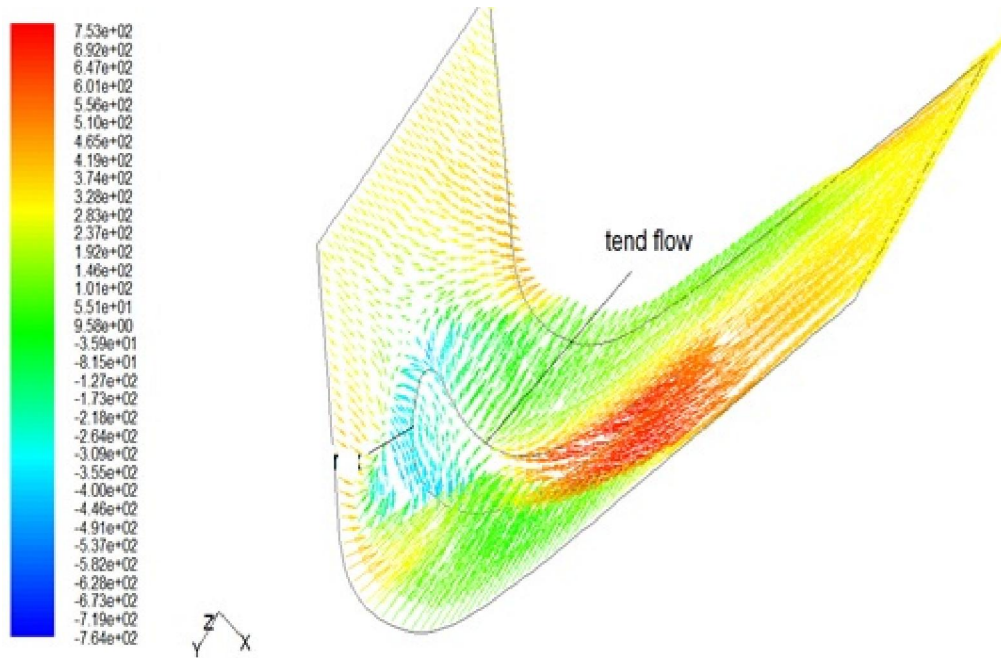
Fig.4.2 Velocity Vector on tip of Blade at rotation speed 3500 rpm for tip clearance (a) 4mm (b)6mm.

## 4.4 Flow feature inside tip clearance

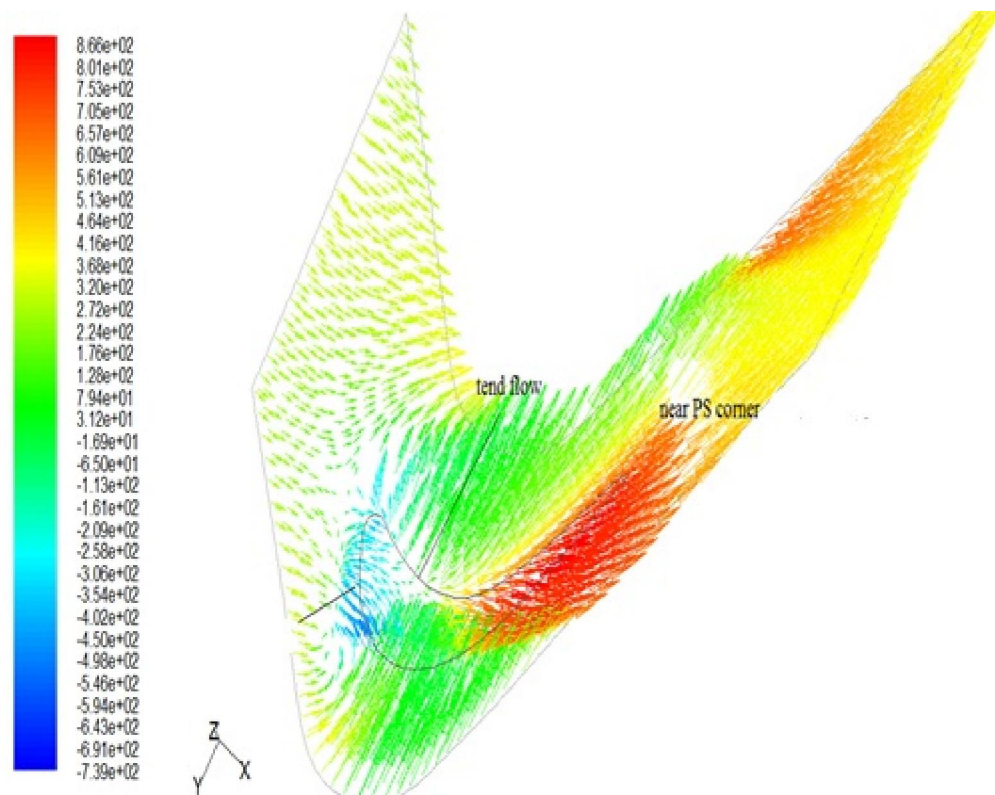
In order to visualize the typical tip leakage flow structure, a 3-D view of velocity vector and path lines are adopted in Figure.4.3 and figure.4.4 for both tip clearance (4 mm) and tip clearance (6mm) cases at rotation speed.

### 4.4.1 Velocity Vector.

The velocity vectors on the blade-to-blade surface near the tip are presented in Figure. 4.3. This figure shows how the flow leaking through the tip clearance gap moves away from the blade suction surface. This leakage flow interacts with the overturned end wall flow near the suction surface and rolls down from the end wall to form a leakage vortex. This figure indicates, there is little change in the flow direction from the pressure side to suction side, except near the blade Leading edge. The flow splits when approaching the leading edge. It flows either to the suction side of the blade as the common overturning of the end wall flow or across the gap from the pressure side to the suction side of the next blade as it merges with the end wall flow from the next passage forming the leakage vortex.



(a)



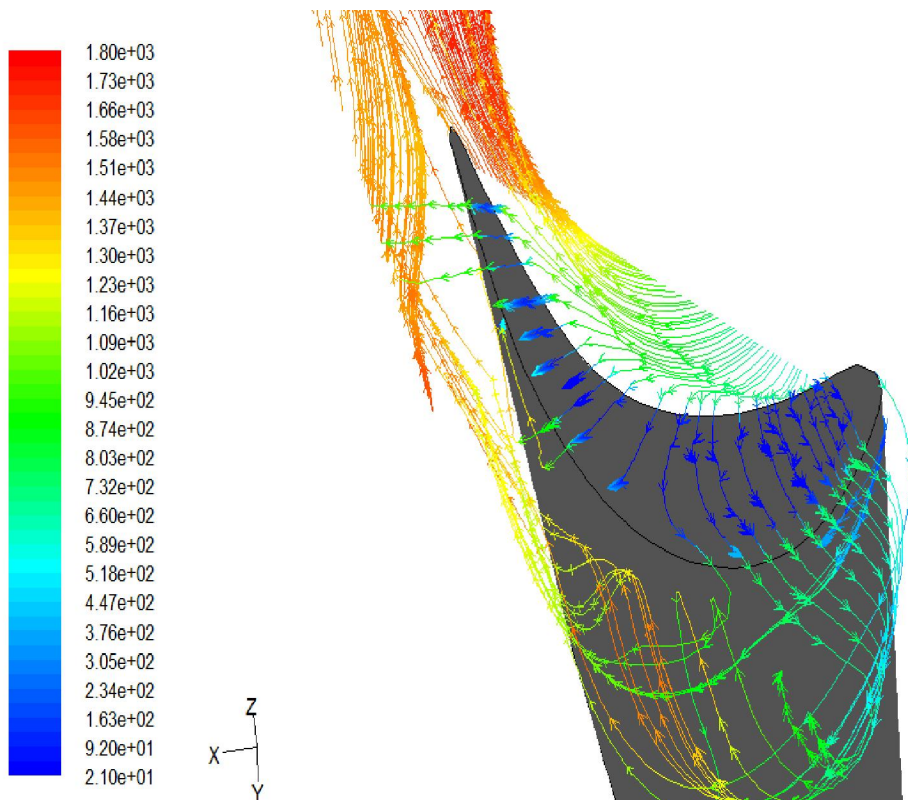
(b)

Fig.4.3 Velocity Vector at plane near the tip of blade for tip clearance (a) 4mm, (b) 6mm.

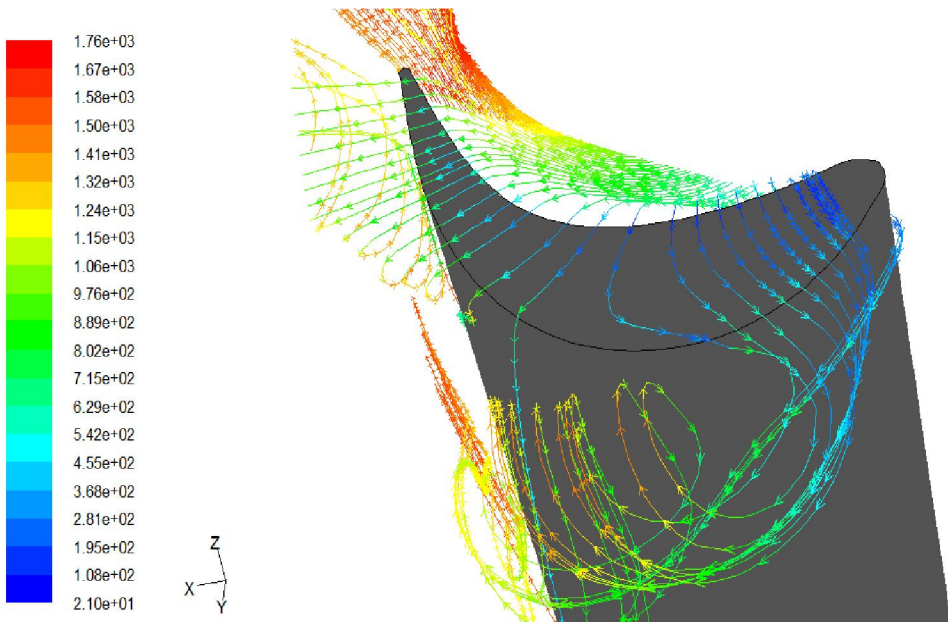
#### 4.4.2 Flow particles Traces inside the Tip Clearance Region.

Figure.4.4 shows particle traces released from points inside the blade-to-blade passage for both T.C (4mm), and T.C (6mm) cases. This figure shows fluid path lines at 3500rpm. The size of the leakage vortex is clearly larger for the tip clearance (6 mm) case, due to the greater mass flow rate leak through the tip clearance .this figure explains the effect of tip clearance size. Leakage flow jet starts from the leading edge of rotor blade for both tip clearance cases and it ends to about 65 percent of blade tip chord from T.E or the tip clearance (4mm) case and to 74.9 percent of blade tip chord for the tip clearance (6mm) case. Figure.4.4 also show the existence of path lines from the nearby blade for the T.C=6 mm case. This is due to strong tip leakage vortex and larger mass flow rate. The flow from nearby blade may interact with passage flow further downstream and may contribute to disturb the flow.

Particle traces released from different radius on passage are shown in Figure.4.5. Figure.4.5 (a) shows that the leakage flow exists for both two tip clearance cases when the particles are released from 76 percent inside passage on pressure side while there is no existence of leakage flow for particles that released from radius smaller than 76 percent inside passage. Figure.4.5 (b) also shows that the leakage flow through the tip clearance generates tip leakage vortex for T.C 6mm case while this leakage flow for T.C 4mm case does not generate tip leakage vortex. Figures 4.5 (c, d and e) explains being of tip leakage flow and tip leakage vortex for both T.C=4mm and T.C 6mm cases. The tip leakage vortex size becomes larger and its size becomes wider for the particles that are released from radius inside passage on pressure side near the tip clearance region. These figures also show that the fluid particles were strongly rolled up for T.C 6mm case than that for T.C 4 mm case. This can be clearly seen in Figure.4.5 (e).



(a)



(b)

Fig.4.4 Fluid Path Lines Through Different Tip Clearance at 3500rpm

(a) 4mm (b) 6mm

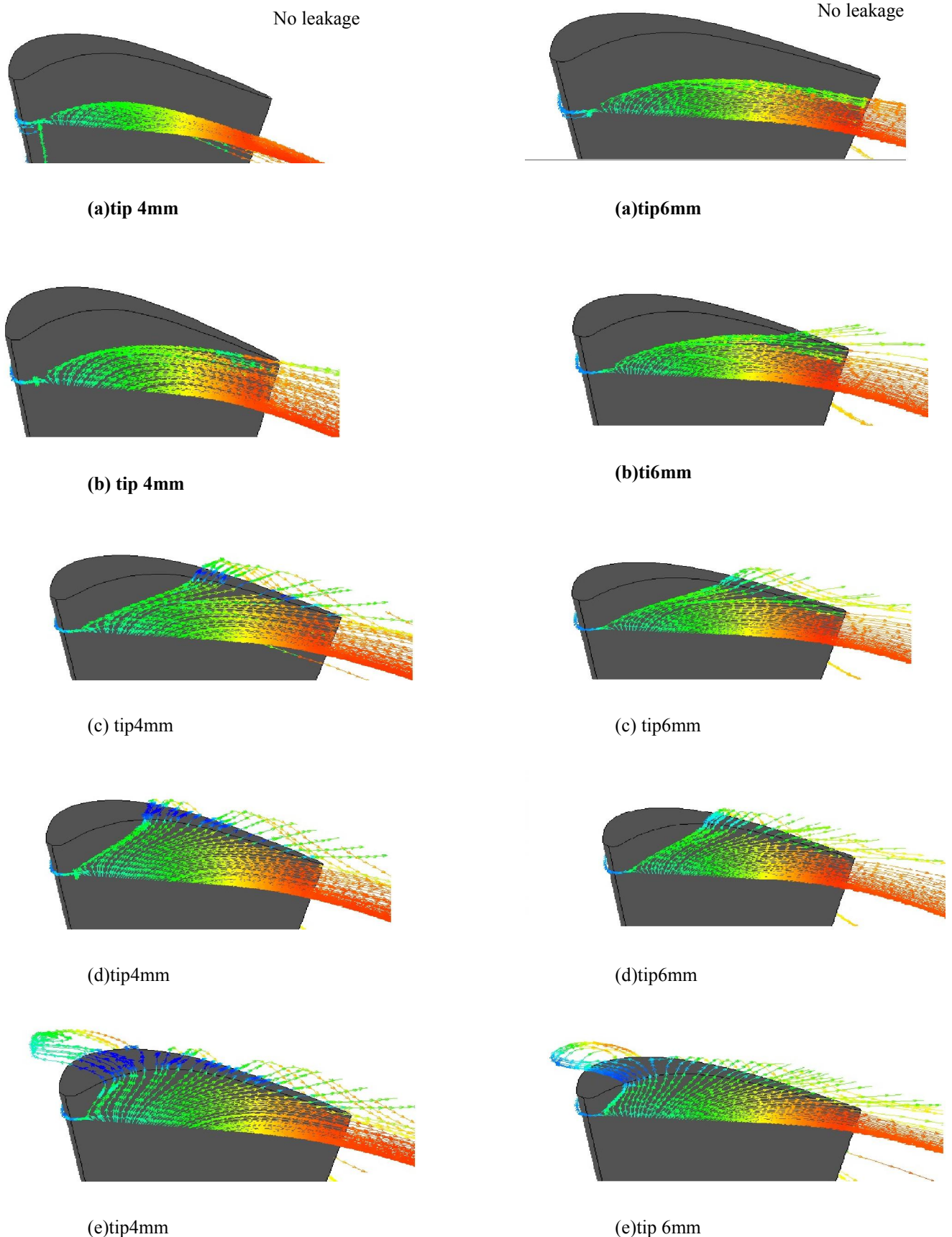
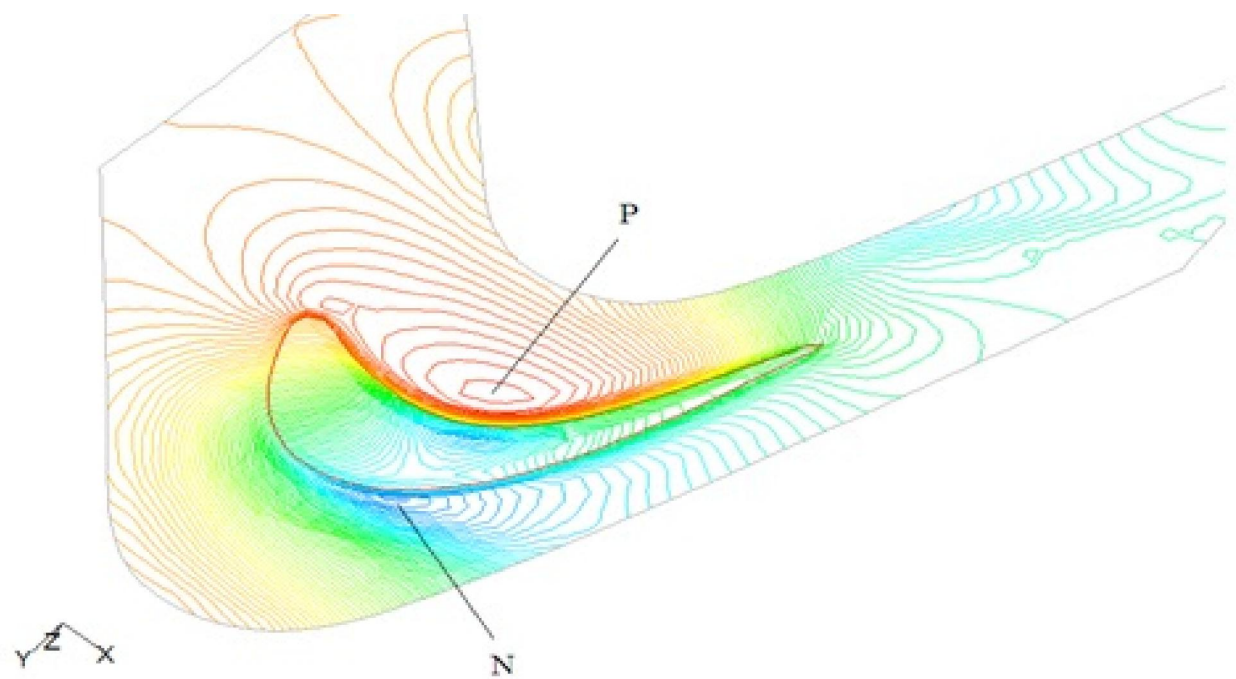


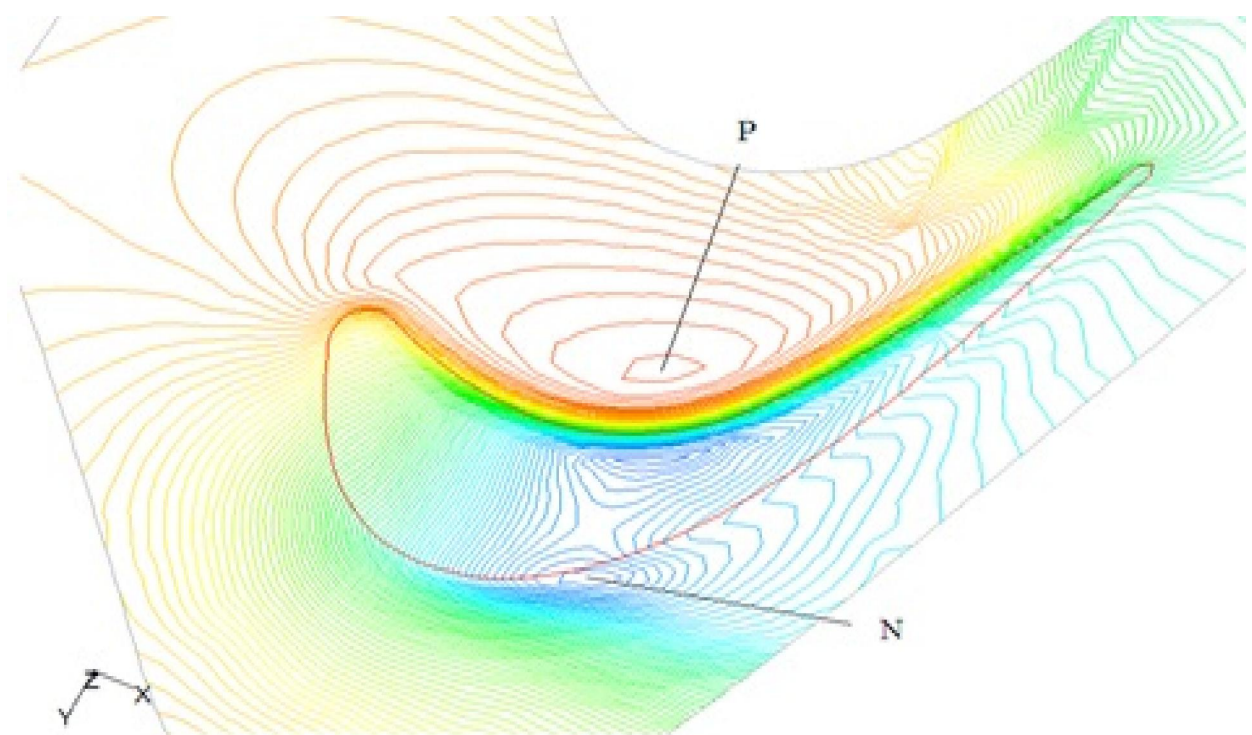
Fig.4.5 Particle Traces Through tip clearance Released From Different radius inside passage on the Pressure Side (a) 76% (b) 78% (c) 82% (d) 86 % (e) 88% .

## 4.5 Determination of tip leakage vortex core locations at different speed

The pressure distribution on the surface inside tip clearance region at different tip clearance sizes and for different rotation speed are shows in Figure.4.6.and figure.4.7. As shown in these figure, a deep pressure depression exists near the suction side denoted by point (N). This deepest pressure indicates an existence of strong leakage flow or tip leakage vortex generated in that region. Point (P) show that the highest static pressure on pressure side. due to this high difference in pressure the flow leak through tip clearance from pressure side to suction side and causes an existence of strong rolling up effects and large losses in that region. These figures indicate that, as tip clearance increases the location of tip leakage vortex core moves at higher rotation speeds to the leading edge (L.E). These figures also indicate that the region of existence of vortex for tip clearance =6mm case is larger than that for tip clearance =4mm case at some speed .it seen in figure .4.7.

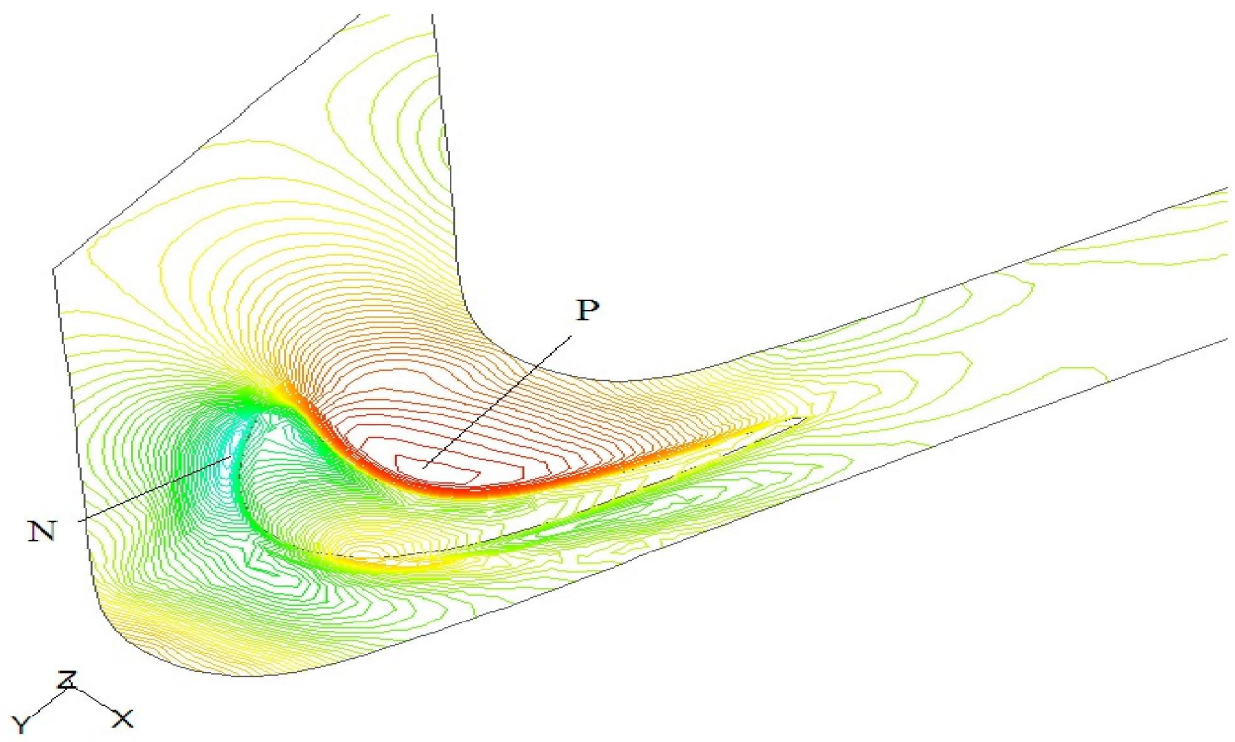


(a)

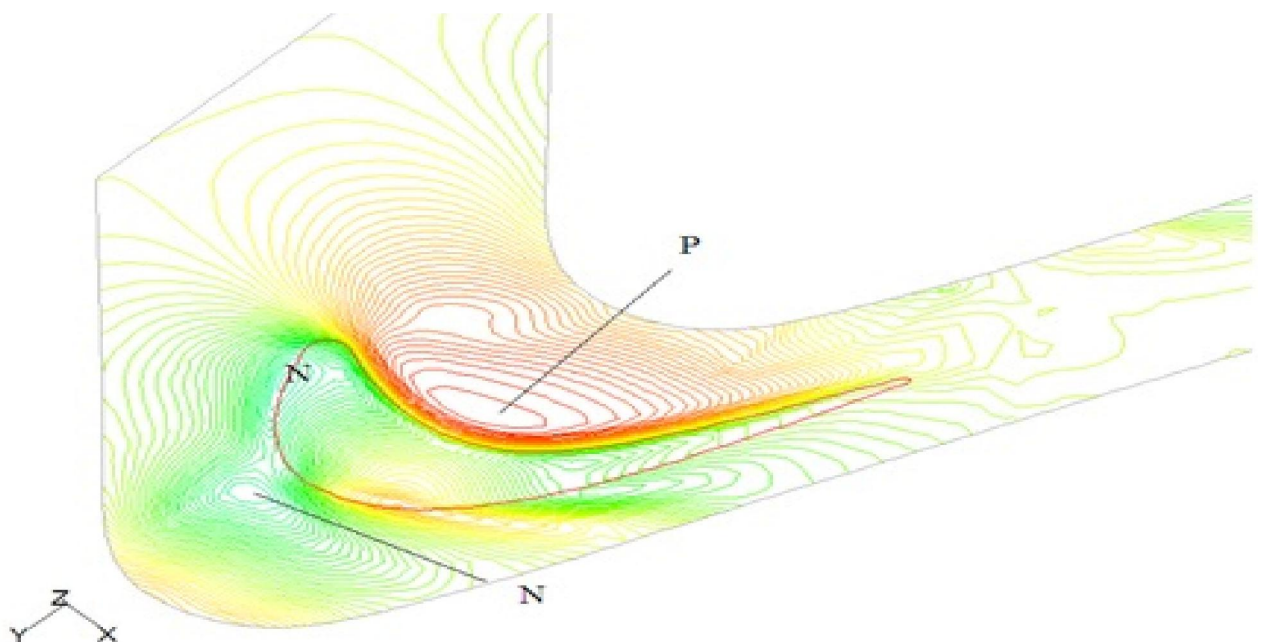


(b)

Fig.4.6 contour of static Pressure distribution on surface inside tip region at 1000rpm  
(a) 4mm (b) 6mm.



(a)



(b)

Fig.4.7. contour of static pressure on surface in side tip regain at 3500rpm.(a) 4mm (b) 6mm

## 4.6 Determination of tip clearance effects on vortex and wake flow.

Figure.4.8.(a)and figure.4.9.(b) show the axial velocity at different radial locations. On passage the region of axial velocity at tow tip sizes (4mm,6mm) sudden decrease occurs at wake range. That drop in axial velocity occurs in wide region near the tip clearance. This to shows that the axial velocity decreases and it may arrived at its minimum value as traveling from mid-span towards the tip clearance region due to effects of tip leakage flow, for both tip clearance. The decrease in axial velocity in the leakage vortex region is due to existence of low energy fluid particles that accumulated near the tip region. These low energy fluid particles move through the tip clearance and form the tip leakage vortex. And also in figure 4.8. (c) show the reduction in axial velocity at different tip clearance size. That show the reduction of axial velocity at tip 6mm large than other .and also in figure.4.8 (d) to show the velocity component for tip 6mm an existence of the wake which can be predicted by a sudden reduction in axial velocity and an increase in tangential velocity. In figure.4.9 show the strength of vortex flows vorticity increase at the cases near tip larger than the vorticity at near hub and at mid span.

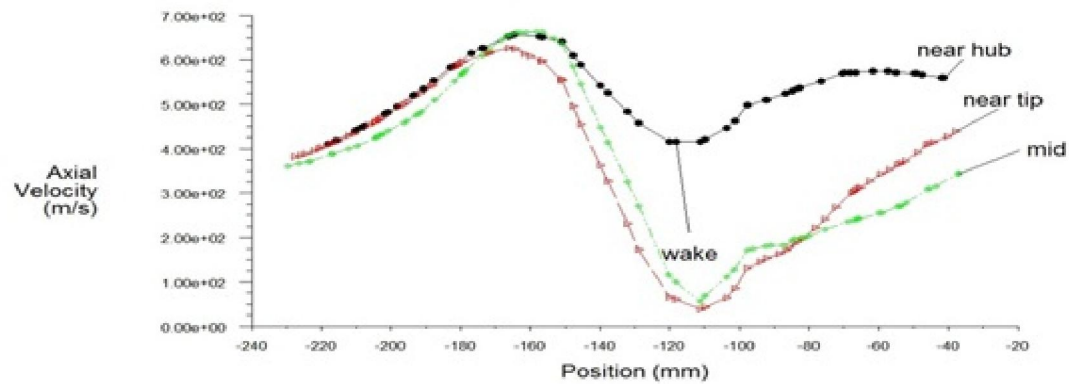


Fig4.8(a)

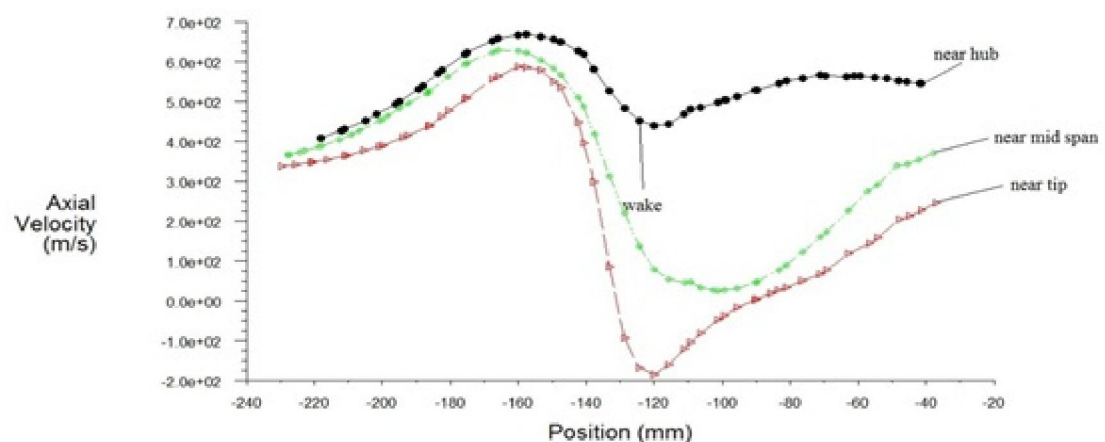


Fig4.8.(b) Axial Velocity tip 6mm at different location .in passeg

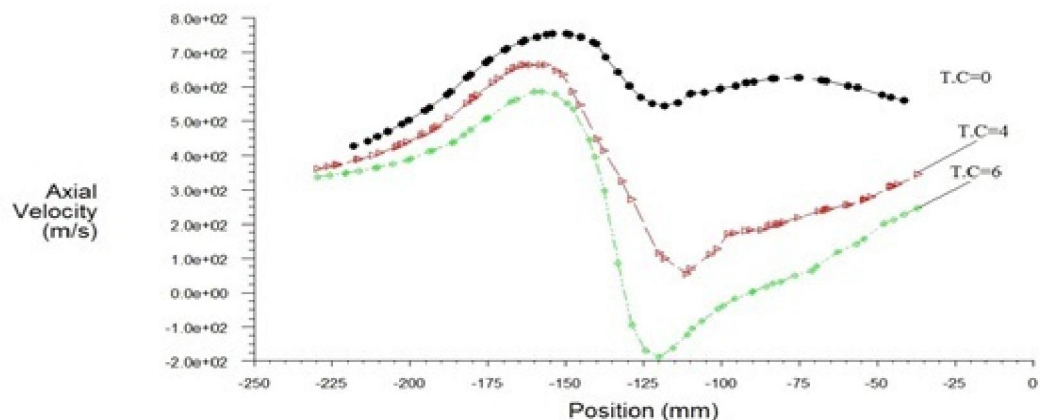


Fig.4.8(c) Axial Velocity at Different Tip Clearance size (T.C=0,T.C=4mm, and T.C=6mm) near tip case

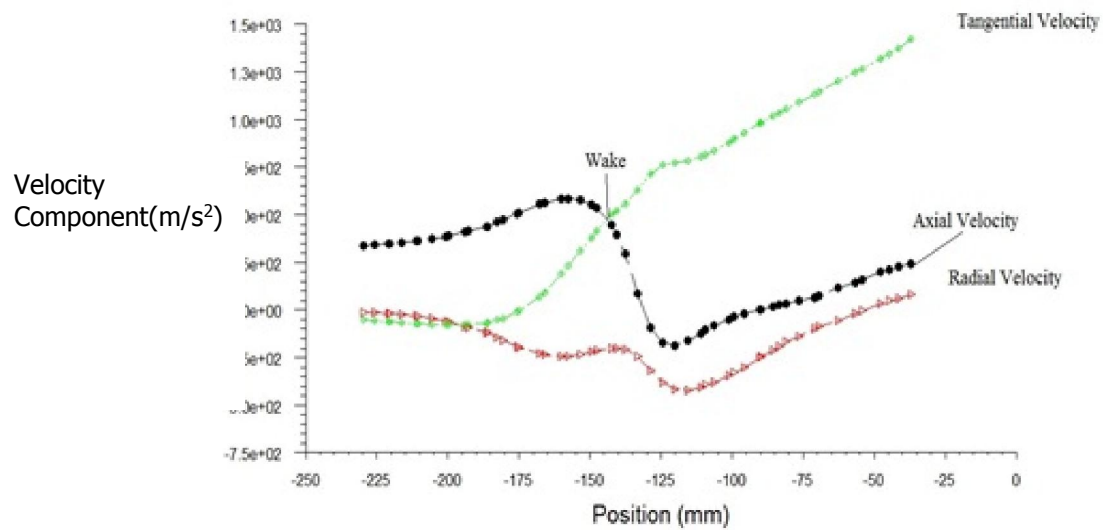


Fig.4.8(d) Velocity component near tip at tip6mm

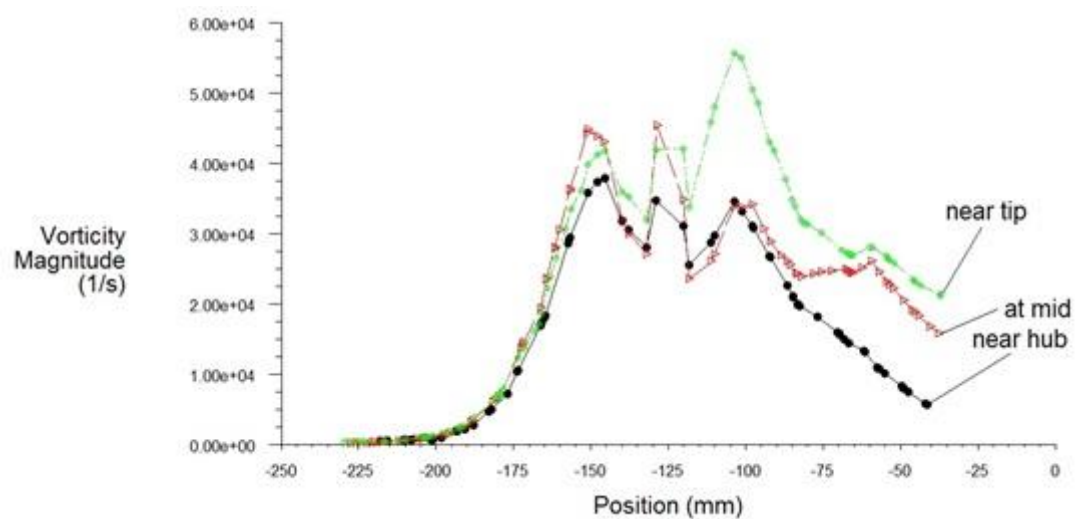


Fig.4.9 Vorticity Magnitude at different distance near case , mid pasege ,and near hub.

# Chapter 5. CONCLUSIONS AND RECOMMENDATIONS

## 5.1 CONCLUSIONS

Present research used numerical simulation techniques to study and analyze the phenomena of tip leakage flow inside axial flow rotor. Three-dimensional flow through axial flow rotor turbine is investigated taking the effect of tip leakage flow on axial flow rotor Performance. Different tip clearance sizes at different rotation speeds are studied using computational fluid dynamics(CFD), the analysis is done using Commercial software fluent based on solving Reynolds Navier -Stokes equations coupled with (  $k-\epsilon$  ) turbulent model. The results from CFD calculations show clearly the influence of the tip clearance and its tip clearance to increase from 4mm to 6mm on the efficiency and total pressure on axial flow rotor. Also It is found through this study the structure of flow inside in side tip clearance for  $T.C=4$  and 6 mm generates a vortex which has an opposite direction to the passage vortex. The size of the vortex increases as the tip clearance gap increases. Also rotation speed has great influence on the tip vortex. It has been found that as rotation speed increases the strength of the tip vortex increases. The wake and core locations it is also are highly influenced by tip clearance and rotation speeds that as tip clearance size increases and rotation speeds the wake becomes weaker.

## 5.2 RECOMMENDATIONS

\*The present study deal with steady simulations to study the effect of tip leakage flow on the performance of the axial flow rotor, the suggestion is to study the effects of tip leakage flow on rotor performance deal with unsteady simulations.

\*In the present study the analysis is carried out using CFD software FLUENT. In the future the analysis can also be carried out by using other CFD software like STAR-CD, ANSYS –CFX, ANSY- ICEM, and COMSOL Multiphysics.

\*Use experimental technique to predict the phenomena of tip leakage flow on the rotor to validate this study.

\*Investigate the heat transfer distributions and the leakage flow structures in the tip region for a plain tip surface at different tip clearance.

\* The flow field downstream of a rotor is strongly influenced by tip leakage vortices and the interaction between these vortices and the surrounding flows can be a significant source of noise. The suggestion to study the effect of the tip leakage flow on downstream flow.

## REFERENCES

[1] Denton, J.D., Dawes, W.N., 1999, Computational Fluid Dynamics for Turbomachinery Design, Proceeding of the Institution of Mechanical Engineers, Journal of Mechanical Engineering Science, Vol. 213, No.C2, pp.107-124

[2] B. Lakshminarayana. Fluid Dynamics and Heat Transfer of Turbomachinery. John Wiley & Sons, Inc., 1996. New York, NY.

[3] J. Bindon. The measurement and formation of tip clearance loss. ASME J. of Turbomachinery, 111:257–263, 1989. 88-GT-203.

[4] U.J.Patdiwala, H.C.P at el, and Paresh K. Parmar , .A Review on Tip Clearance Flow and Secondary Flow Losses in Linear Turbine Cascade, IOSR Journal of Mechanical and Civil Engineering (IOSR-JMCE), Vol. 11, Issue 3, PP 33-37, May-Jun. 2014

[5] Langston, L., S., 1980, Cross flows in a Turbine Cascade Passage, Journal of Engineering for Power, Vol.102, pp.866-874.

[6] J. Tallman and B. Lakshminarayana.Numerical simulation of tip leakage flows in axial flow turbines, with emphasis on flow physics: Part 1 - effect of tip clearance height. ASME Journal of Turbomachinery, 123:314, 2001.

[7] Adams, N.G., and Hepworth, H.K., Flow Visualization Study of Tip Leakage Flows Across Cantilevered Stator Blades,"AIAA Journal of Propulsion, Vol. 4, No. 2, 1988, pp. 144 151.

[8] Cleverson Bringhenti and Joao Roberto Barbosa,2008, “Effects on turbine tip clearance on gas turbine performance

[9] Anderson Jr., J.D.,1995, ”Computational Fluid Dynamics – The Basics with Applications”, McGraw-Hill Series in Mechanical Engineering, Inc. New York, USA, 563 p.

[10] Krishnababu, S. K., 2009,”Aero thermal Investigations of Tip Leakage Flow in Axial Flow Turbines—Part I: Effect of Tip Geometry and Tip Clearance Gap”, ASME, Journal of Turbomachinery, vol. 131, pp. 1-14.

[11] Muthanna, C., 1998, Flow field Downstream of a Compressor Cascade with Tip Leakage, Thesis Submitted to the Faculty of the Virginia Polytechnic Institute and

State University in Partial Fulfillment of the requirements for the degree of Masters of Science in aerospace Engineering William J. Davenport

[12] RajeshYadav, Vishal Gulati & Puneet Katyal ,Investigations of Gas Turbine Characteristics by Varying Tip Clearance and Axial Gap, International Journal of Engineering Research and Applications (IJERA)" Vol. 1, Issue 3, pp.1058-1064

[13] J.S. Liu and R. Bozzola, Three-Dimensional Navier-Stokes Analysis of the Tip Clearance Flow in Linear Turbine Cascades, 31 st Aerospace Sciences Meeting & Exhibit January 11-14, 1993 / Reno, NV, AIAA-93-0391

[14] Krishnababu, S. K., 2009,"Aero thermal Investigations of Tip Leakage Flow in Axial Flow Turbines—Part I: Effect of Tip Geometry and Tip Clearance Gap", ASME, Journal of Turbomachinery, vol. 131, pp. 1-14.

[15] Sell, M., Treiber, M., Casciaro, C. and Gyarmathy, G., 2000,"Tip-clearance-affected Flow Fields in a Turbine Blade Row," Proc. Inst. Mech. Eng., Vol.213, Part A, pp.309, 318.

[16] Ameri, A.A., Steinthorsson, E., Rigby, L.D., 1998, "Effects of Tip Clearance and Casing Recess on Heat Transfer and Stage Efficiency in Axial Turbines," Nasa Contract Report NASA/CR-1998-208514.

[17] Wu, k., Elhadi, E., E., 2003, Simulation of Tip leakage flows and their effects in Axial Flow fan using computational Fluid Dynamics, The 7<sup>th</sup> Asian International Conference on Fluid Machinery, Fukuoka, Japan.

[18] Keith, M., B., 2001, An Improved Streamline Curvature Approach for Off-Design Analysis of Transonic Compression Systems, Ph. D. thesis in mechanical engineering, Blacksburg, Virginia.

[19] Adamczyk, J., J., 1999, Numerical Simulation of Multi-Stage Turbomachinery Flows, Design Principles and Methods for Aircraft Gas Turbine Engines, RTO-MP-8, pp.21-1-21-25

[20] Tallman, J.A., 1999, Simulation of Tip Leakage Flows in Turbine Rotor using Computational Fluid Dynamics, M. Sc. Thesis in Mechanical Engineering, Pennsylvania State University

European Congress on Computational Methods in Applied Sciences and Engineering

[21] Khalid,S.A., Khalsa,A.S., Waitz,I.A., Tan, C.S., Greitzer, E.M., Cumpsty,N.A., Adamczyk, J.J., and Marble, F. E.,1999, "Endwall Blokage in Axial Compressors, ASME Journal of Turbomachinery", Vol. 121, 499-509.)

[22] Tomita, J.T.; Barbosa, J.R., 2011. Influence of Inflow Turbulence Intensity Variations in an Axial Turbine Using 3D Rans Computations. ITA. São José dos Campos, SP, Brazil.

[23] Elhadi, E., E., Wu, K., 2002, Simulation of Vortex Flows in Axial Flow Fan using Computational Fluid Dynamics, Pakistan Journal of Information and Technology, Vol.1, No.3, pp. 242-249.

[24] Moore, J. and Tilton, J.S., A Computational Study of Tip leakage flow in a linear turbine cascade, Journal of Turbomachinery, ASME Transactions, vol. 110, pp. 18-26, 1988.

[25] Suneeesh, S., S., Prasad and Sitaram, N., 2002, Effect of Axial Spacing on the Rotor/Stator Interaction in an Axial Flow Compressor, The Fourth International Conference on Pumps and Fans, Tsinghua University, Beijing, pp.360-367.

[26] Martin,B., 2002, Experimental and Numerical Investigation of a Three Dimensional Boundary Layer in the Region between a Casing and a Blade Tip, The 4th International Conference on Pumps and Fans, Tsinghua University, Beijing pp.87-94

[27] Wilcox, David C (1998). "Turbulence Modeling for CFD". Second edition. Anaheim: DCW Industries, 1998. pp. 174.).

[28] Jones, W. P., and Launder, B. E. (1972), "The Prediction of Laminarization with a Two-Equation Model of Turbulence", International Journal of Heat and Mass Transfer, vol. 15, 1972, pp. 301-314.

[29] Launder, B. E., and Sharma, B. I. (1974), "Application of the Energy Dissipation Model of Turbulence to the Calculation of Flow Near a Spinning Disc", Letters in

[30] Patankar, S. V., 1980, Numerical Heat Transfer and Fluid Flow, Hemisphere Publishing Corporation, Taylor & Francis Group, New York.

[31] Thorpe, S. J., Yoshino, S., and Thomas, G., "Blade Tip Heat Transfer InTransonic Heat Transfer", Journal of power and energy, Vol. 219 part A 2005

[32] FLUENT User's Manual, Fluent. Inc.

[33] Gambit user's manuals.

## Appendix- A

### A .1 Introduction

The purpose of this research is to demonstrate the effect of tip leakage flow on axial flow rotor ,model for analyzing the aerodynamic in 3D axial flow rotor .the tip leakage flow phenomenon in turbomachinery has attracted the attention of researchers in turbomachinery field.

This appendix demonstrates how to do the following:

- Use the axial flow rotor turbine with tip clearance to aerodynamic analyses the effect of tip leakage flow through the tip clearance on the turbine performance.
- Pre-process used Gambit software.
- Problem case Set up and solve the case with appropriate.
- Post process the resulting data.

### A.2 Require :

Calculation of mass flow rate concentration total pressure and losses of flow through the tip clearance ,plot of velocity vector and path line in the tip region to show the leakage flow through the gap.

### A.3 problem description and boundary condition

The problem to be considered as show in the schematically of axial flow turbine in figure 1 .the rotor consist of 60 blade .a steady state solution for this configuration using the rotor blade Pressure at inlet is used at the upstream boundary and the static pressure used at outlet downstream boundary. The periodic boundary rotational and fluid moving reference frame ,turbulent, and steady state flow condition will be considered to solve the flow field.

### A.4 set up problem in fluent solver

Step1Grid.

Step2Units.

Step 3 models.

Step 4 material selection.

Step 5 operation condition.

Step 6 boundary condition.

Step 7 solution.

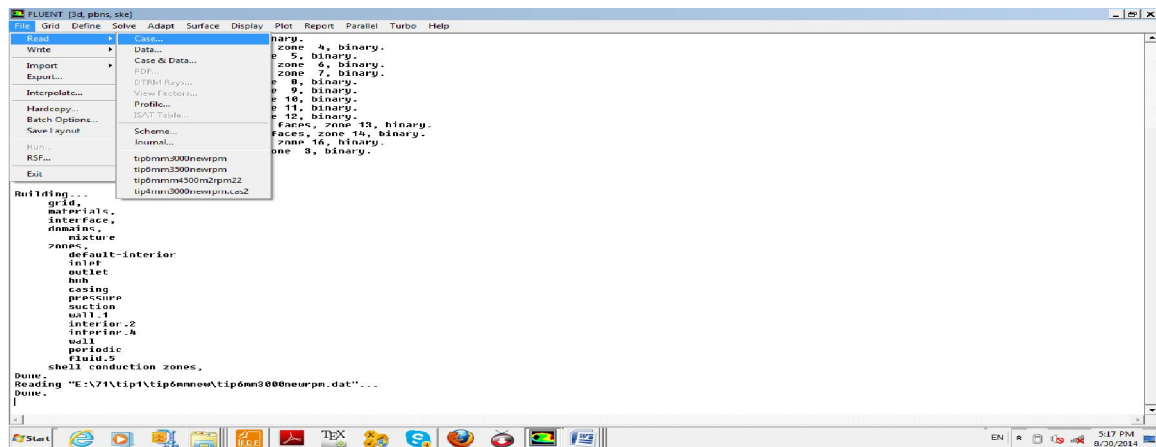
Step 8 post processing.

A.5 preparation

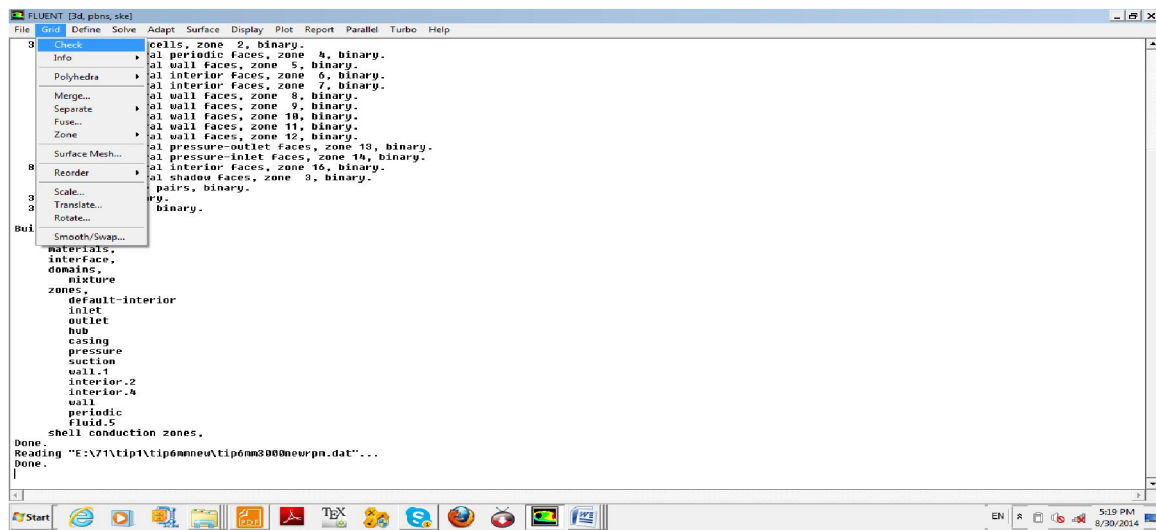
Start the 3D version 6.3.2.6 of fluent

1. Reading and Checking the Grid.

## \*Step1 Grid



2/ Check the grid.



```

FLUENT [3d.pdns.ste]
File Grid Define Solve Adapt Surface Display Plot Report Parallel Turbo Help
Done.
Grid Check
Domain Extents:
  x-coordinate: min (n) = -3.000000e-001, max (n) = 1.000000e-001
  y-coordinate: min (n) = -3.922175e-001, max (n) = 2.969329e-001
  z-coordinate: min (n) = 1.975500e+000, max (n) = 2.295980e+000
Volume statistics:
  minimum volume (n0): 1.321655e-006
  maximum volume (n0): 1.321655e-006
  total volume (n0): 2.399745e-002
Face area statistics:
  minimum face area (m2): 1.029720e-006
  maximum face area (m2): 3.410997e-004
  checking number of nodes per cell.
  Checking number of faces per cell.
  Checking thread pointers.
  Checking number of cells per face.
  Checking boundary types.
  Checking bridge faces.
  Checking right-handed cells.
  Checking zone order.
  Zone 16: 881286 right-handed, 12 left-handed
  Checking face node order.
  Checking element type consistency.
  Checking boundary types.
  Checking face pairs.
  Checking periodic boundaries.
  Zone 4: average rotation angle (deg) = -5.997 (-6.000 to -6.000)
    stored zone rotation angle (deg) = -6.000
    stored axis = (1.000000e-001, 0.000000e+000, 0.000000e+000)
    stored min = (0.000000e+000, 0.000000e+000, 0.000000e+000)
Warning: The mesh contains very high aspect ratio hexahedral or polyhedral cells. The default algorithm used to compute the wall distance required by the turbulence models might produce wrong results in these cells. Please inspect the distance by displaying the contours of the 'Cell Wall Distance' at the boundaries. If you observe any irregularities we recommend the use of an alternative algorithm to correct the wall distance.

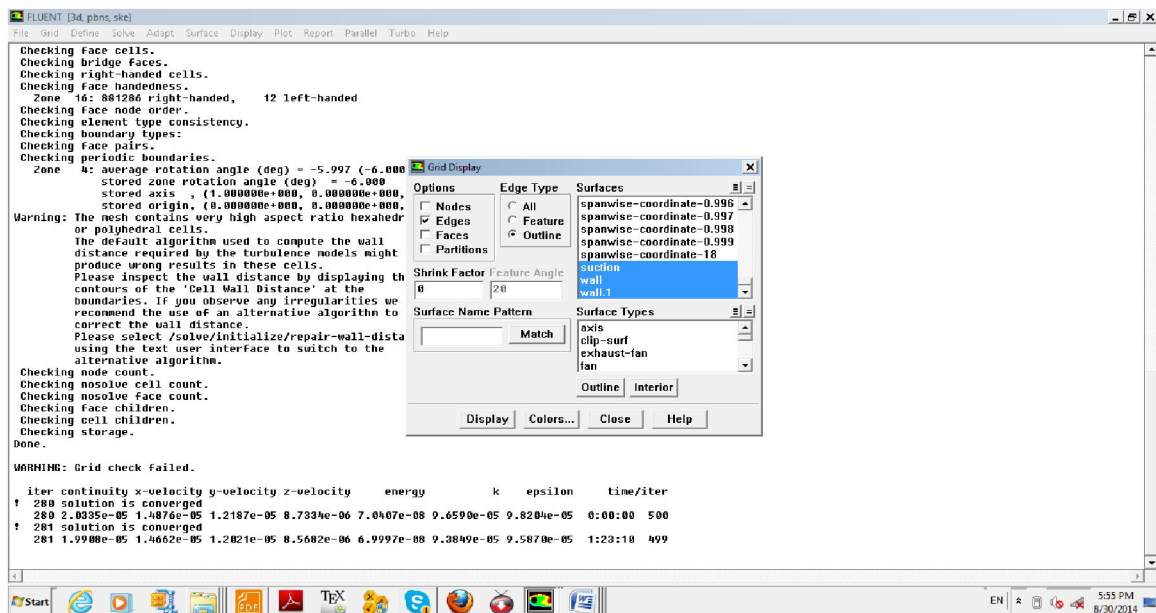
```

FLUENT will perform various checks on the grid and will report the progress in the console window. Pay particular attention to the minimum volume. Make sure that this is a positive number.

### 3. Display the grid (Figure A.2).

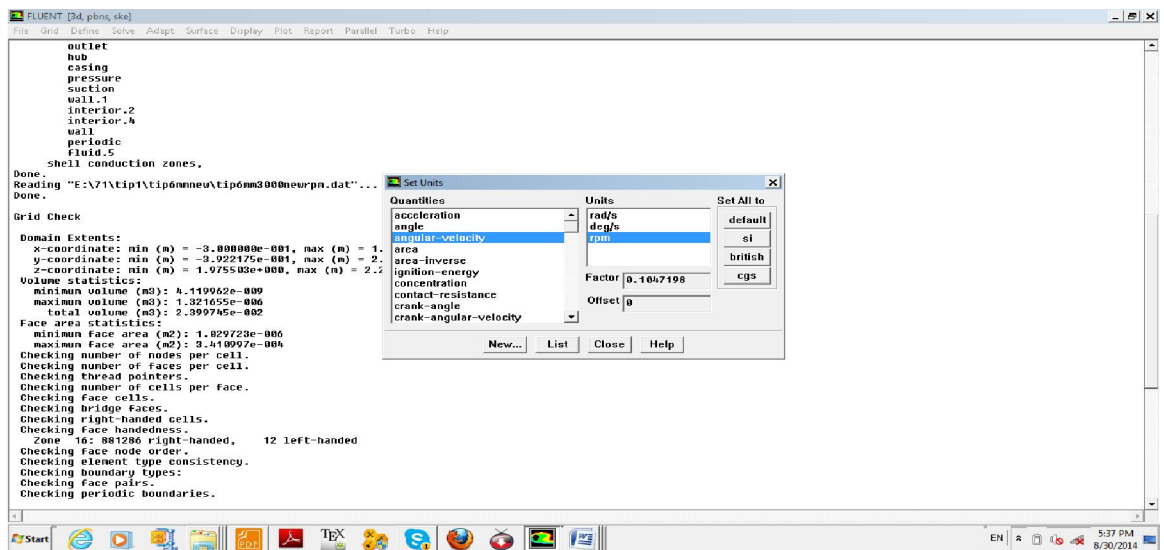


- Select Grid.
- Select display.
- Rotate the view to get the display shown in Figure 3.1



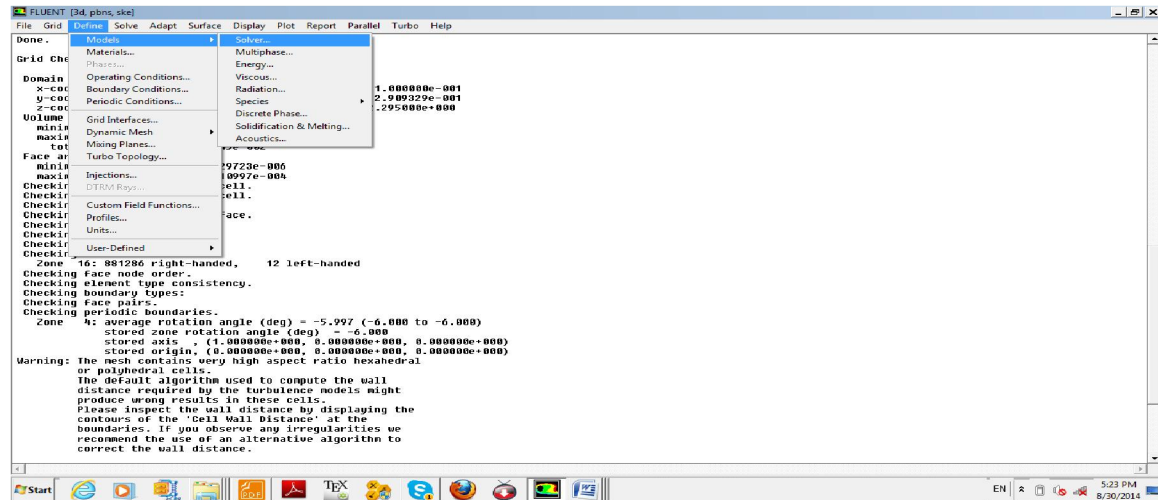
## \*Step 2 Units

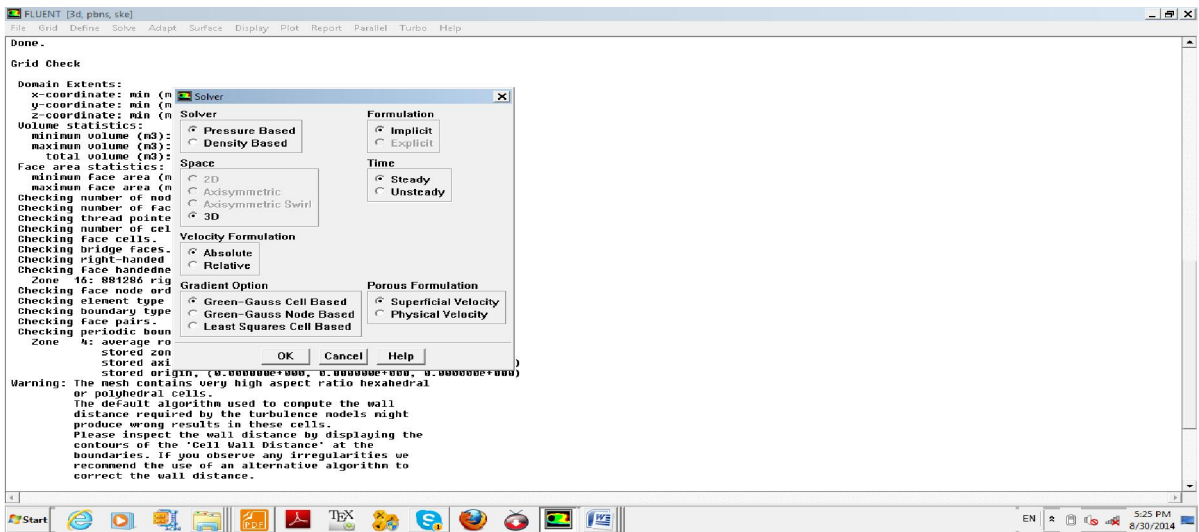
For convenience, define new units for angular velocity. The angular velocity for this problem is known in rpm, which is not the default unit for angular velocity. You will need to redefine the angular velocity units as rpm.



### \*Step3 models

1\ Solver is taken as pressure based and formulation as implicit, space as 3D and time as steady.

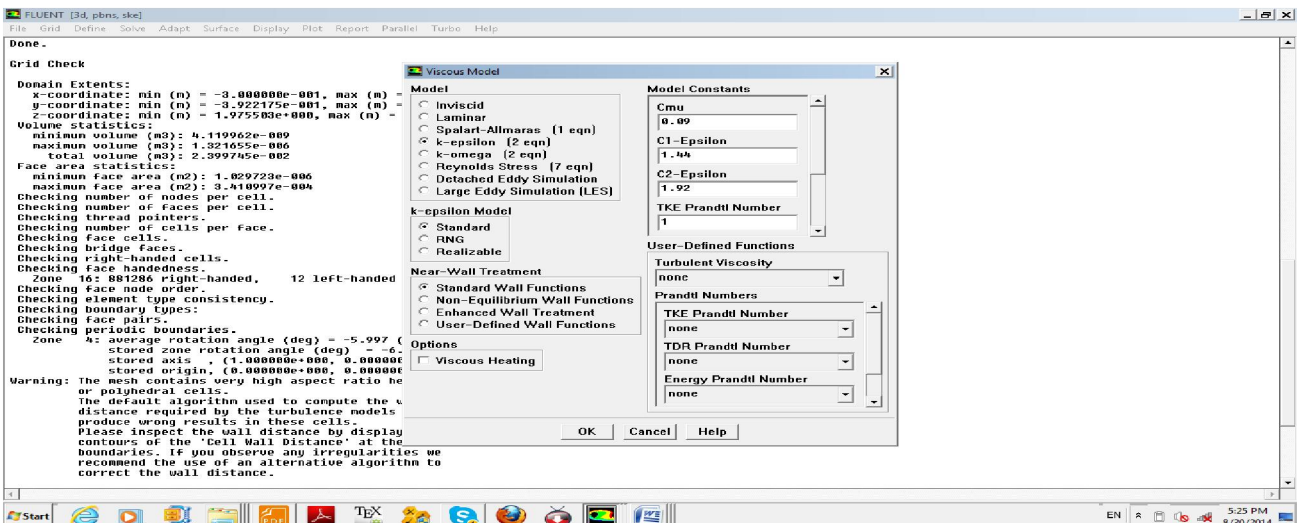




2\ Turn on the standard k- $\epsilon$  turbulence model with standard wall functions.

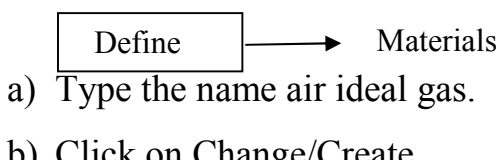


- Under the Model, select k-epsilon.
- Under k-epsilon Model, keep the default Standard option.
- Under Near-Wall Treatment, keep the default Standard Wall Functions option.

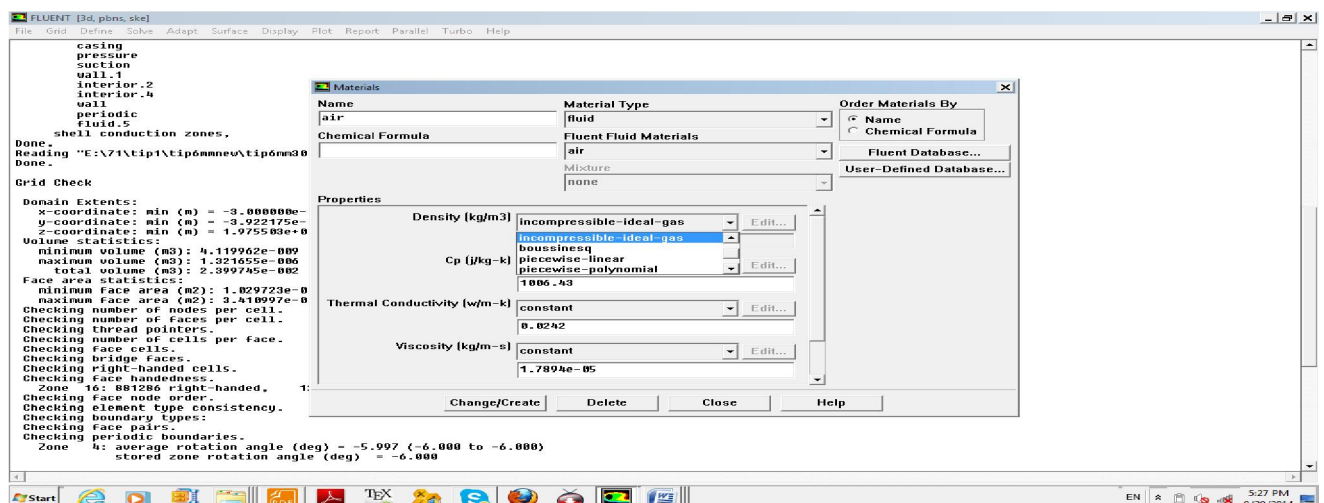
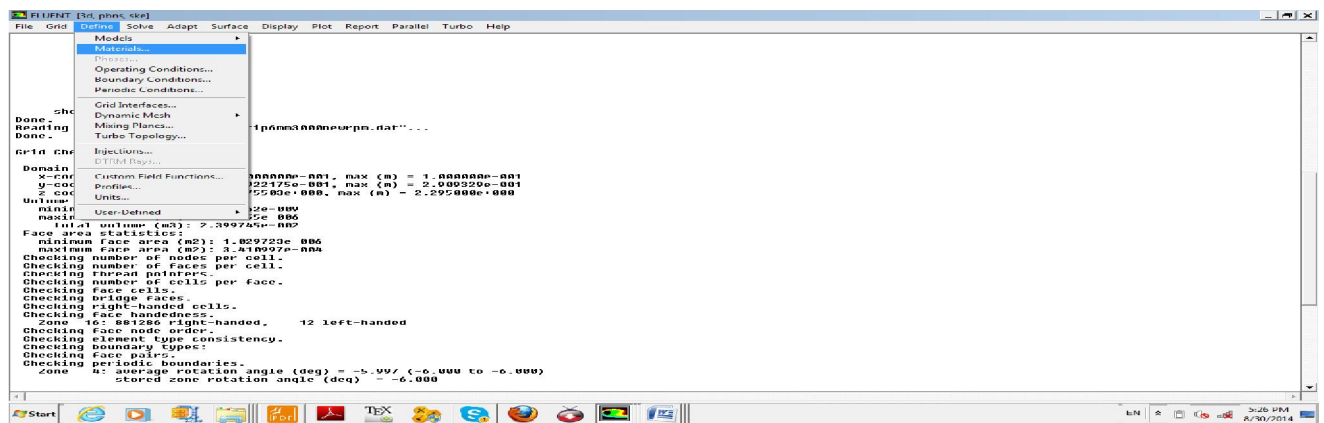


## \*Step 4 Materials

1-Accept the default properties for air.



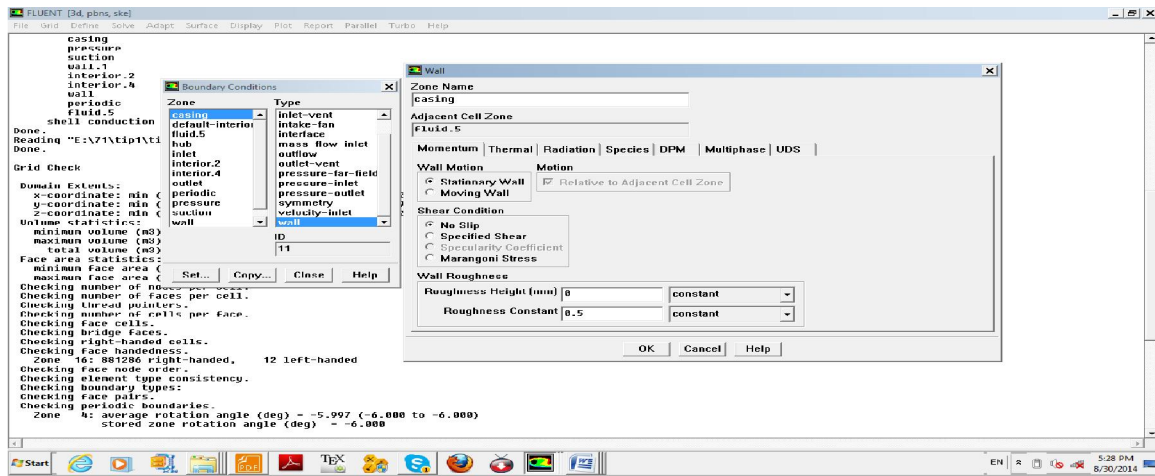
For the present analysis, you will model air ideal gas as an compressible fluid with a density of 1.25666k/m<sup>3</sup> and a dynamic viscosity of 1.789410–5kg/m·s.



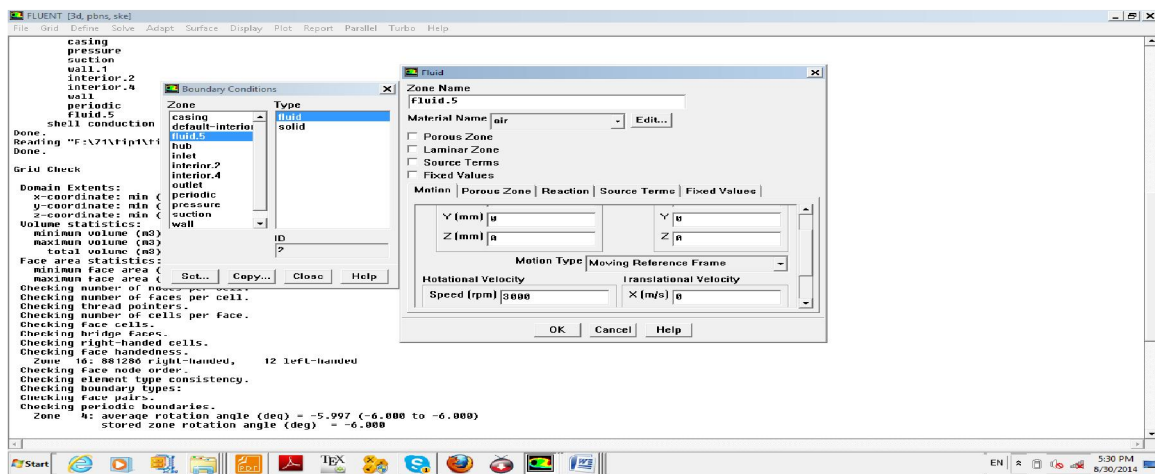
## \*step 5 Boundary conditions



1. Set the conditions for the rotor fluid (fluid-rotor).
  - a) Under Rotation-Axis Direction, enter 1 to X.
  - b) Select Moving Reference Frame in the Motion Type drop-down list.
  - c) Set the Speed (under Rotational Velocity) to 3000rpm.



2. Set the conditions for rotor casing , Accept the default conditions for the rotor-casing .for stationary wall .



3. Set the following conditions for the pressure inlet of the rotor (pressure-inlet).

a) Set the Gauge Total Pressure to 460000Pa.

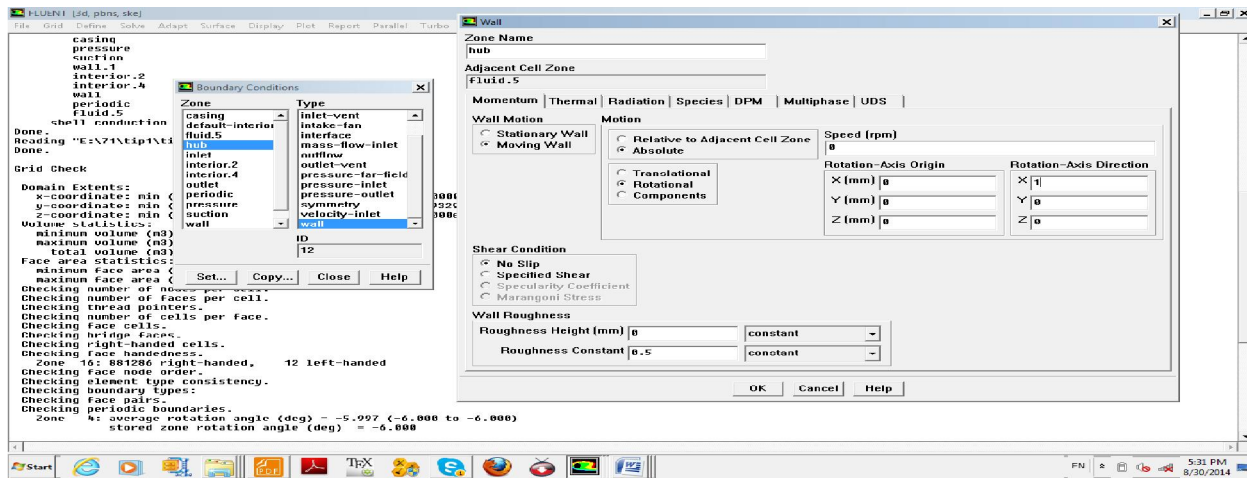
Set the Total Temperature to 444K.

b) In the Direction Specification Method drop-down list, select Direction Vector.

c) In the Turbulence Specification Method drop-down list, select K-epsilon and

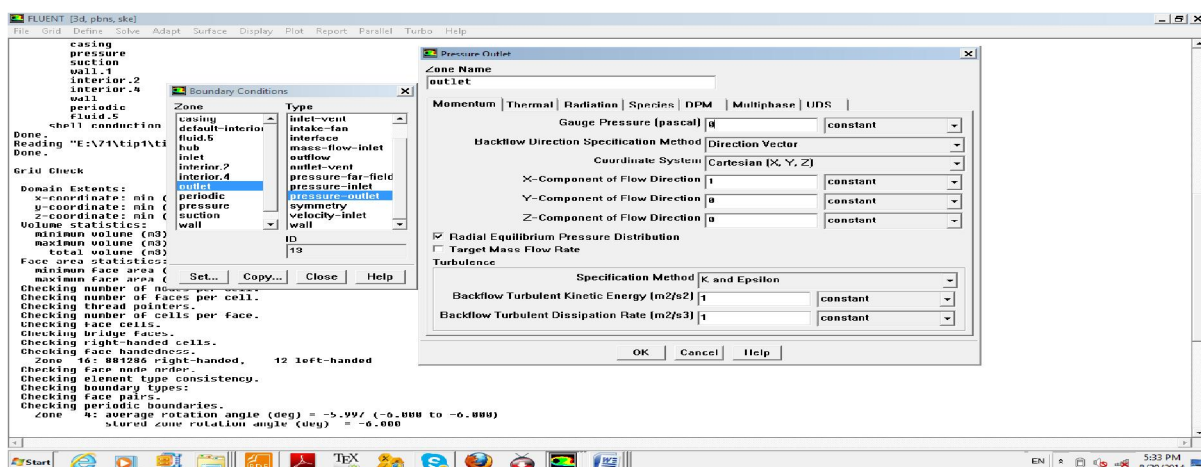
d) Set the Turbulence Kinetic  $1 \frac{m^2}{s^2} 0.5\%$ , and the Turbulence Dissipation

Rate  $1 \frac{m^2}{s^3}$ .



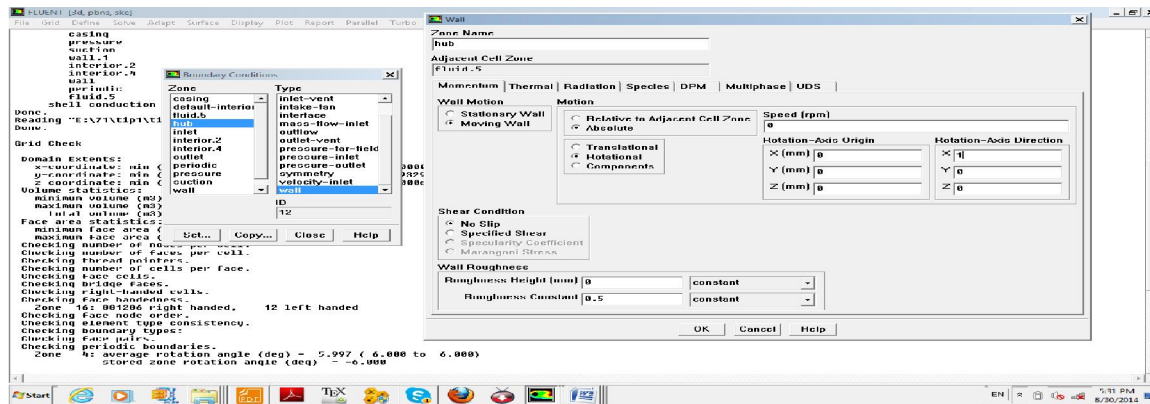
#### 4. Set the conditions for the pressure outlet .

- Set the Gauge Pressure to 146000pa.
- Set the Backflow Total Temperature to 300K.
- In the Direction Specification Method drop-down list, select Direction Vector.
- Select Radial Equilibrium Pressure Distribution.
- In the Turbulence Specification Method drop-down list, select K-epsilon.
- Set the Backflow Turbulence Kinetic Energy to 1%.
- Set the Backflow Turbulent Viscosity Ratio to 1.

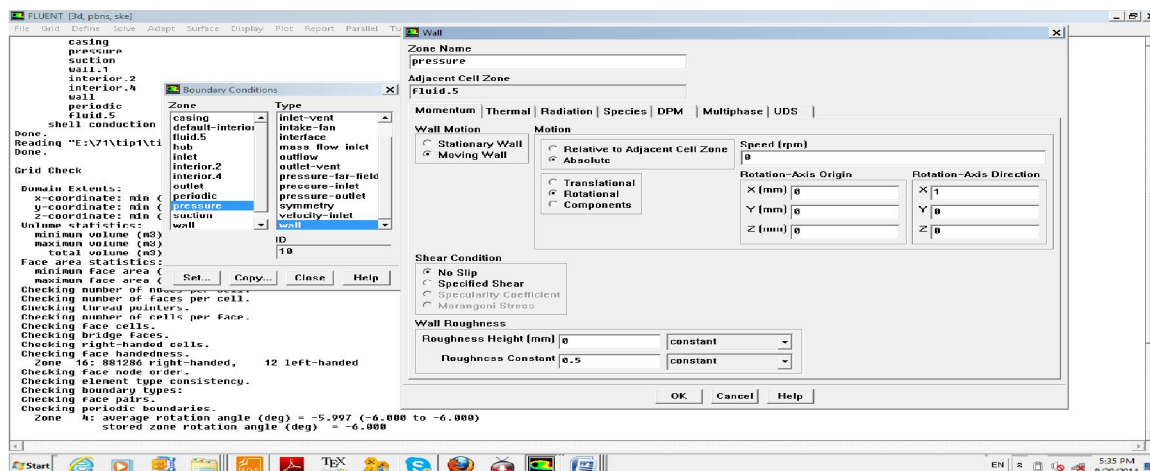


#### 5. Set the conditions for the hub.

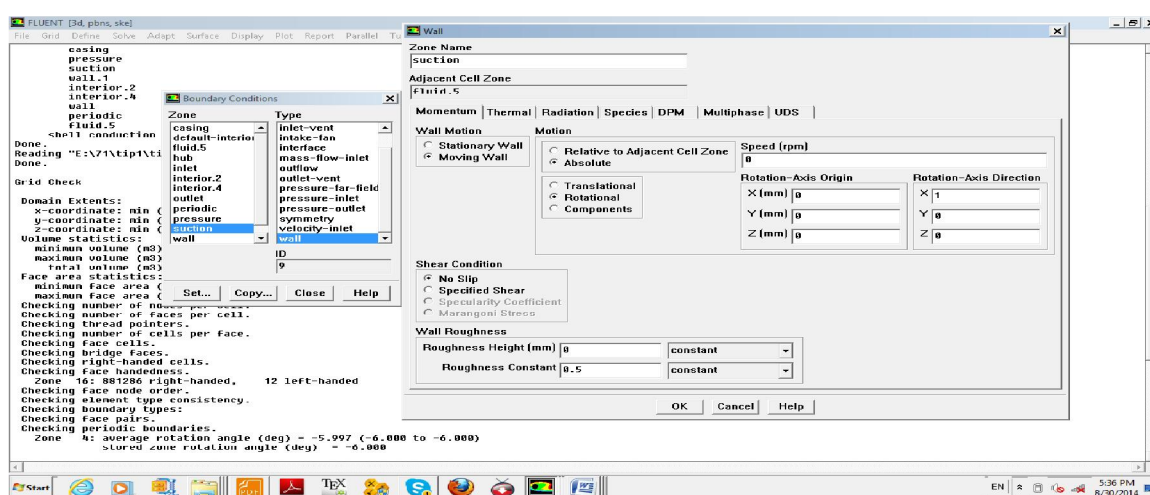
- Select Moving Wall.
- Select Absolute and Rotational under Motion.
- Set the Rotation-Axis Direction by entering 1 to X.



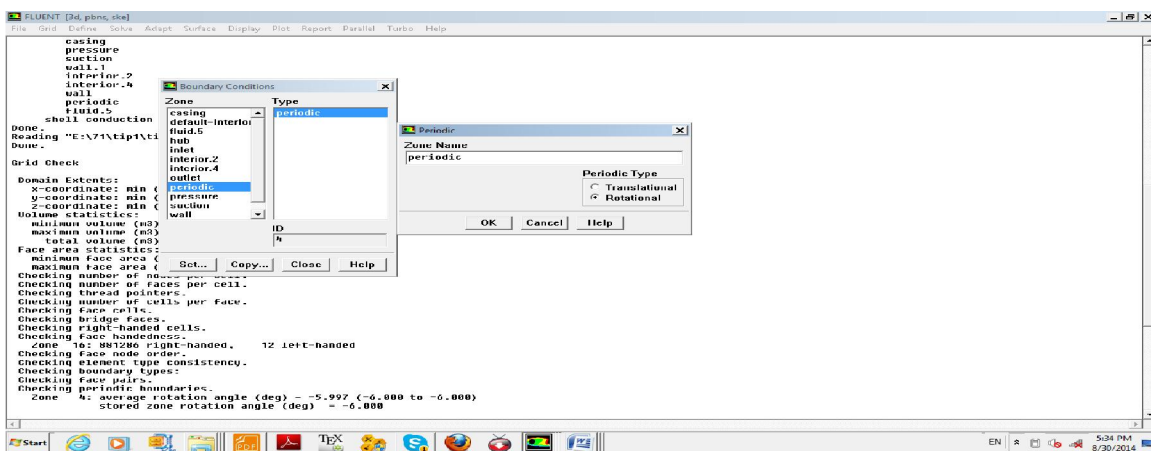
6. Set the conditions for the blade pressure side .
  - a) Select Moving Wall.
  - b) Select Absolute and Rotational under Motion.
  - c) Set the Rotation-Axis Direction by entering 1 to X.



7. Set the conditions for the blade suction side.
  - a) Select Moving Wall.
  - b) Select Absolute and Rotational under Motion.
  - c) Set the Rotation-Axis Direction by entering 1 to X.



## 8. Specify rotational periodicity for the periodic boundary of the rotor.

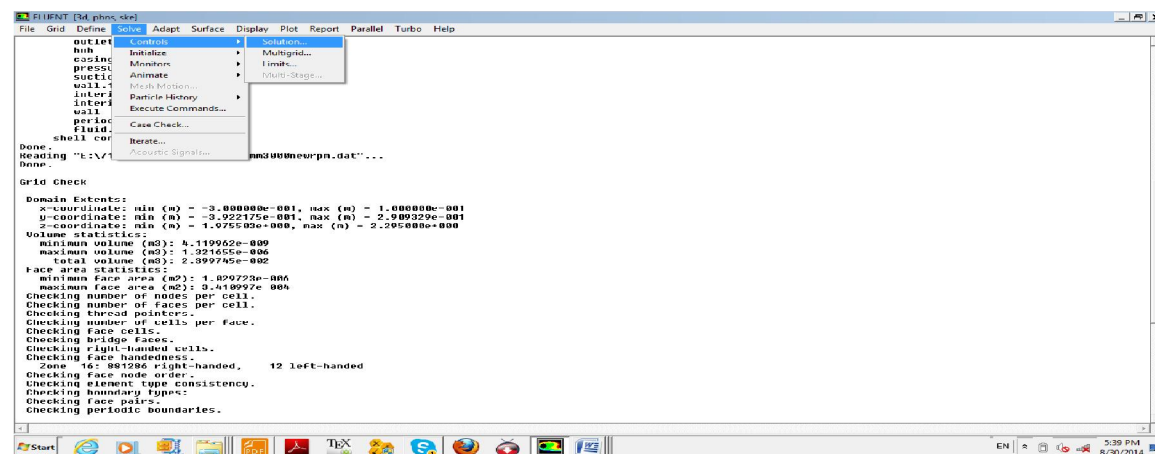


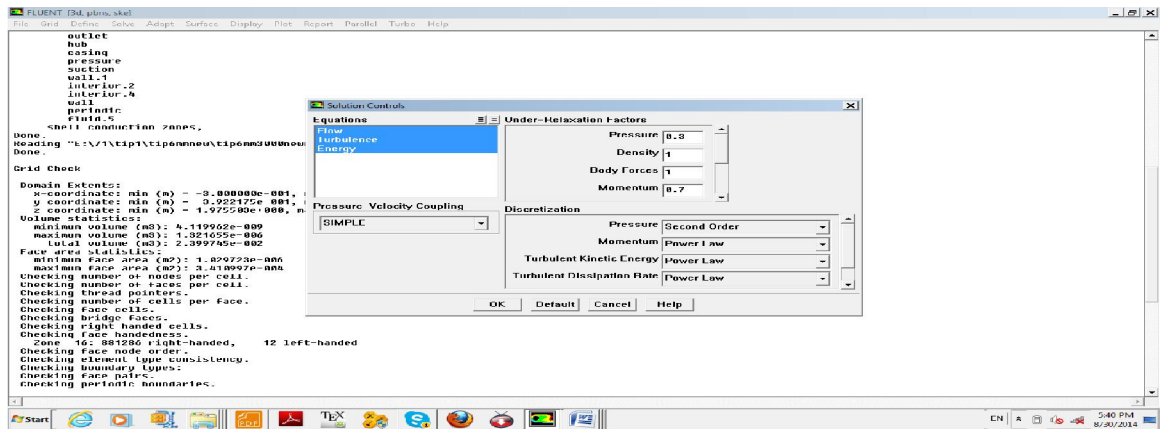
\*step 6 solution



### 1-Under Discretion.

- Select second order upwind for pressure
- Select power law for momentum,Turbulent Kinetic energy ,Turbulent Dissipation Rate ,and Energy.
- Keep default value of Relaxation Factor.





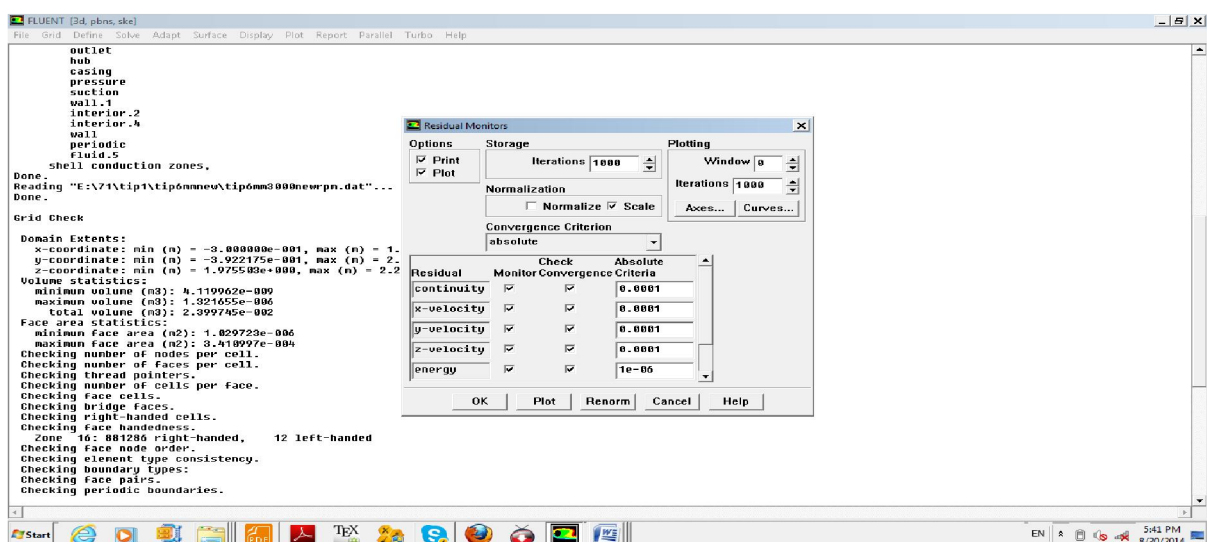
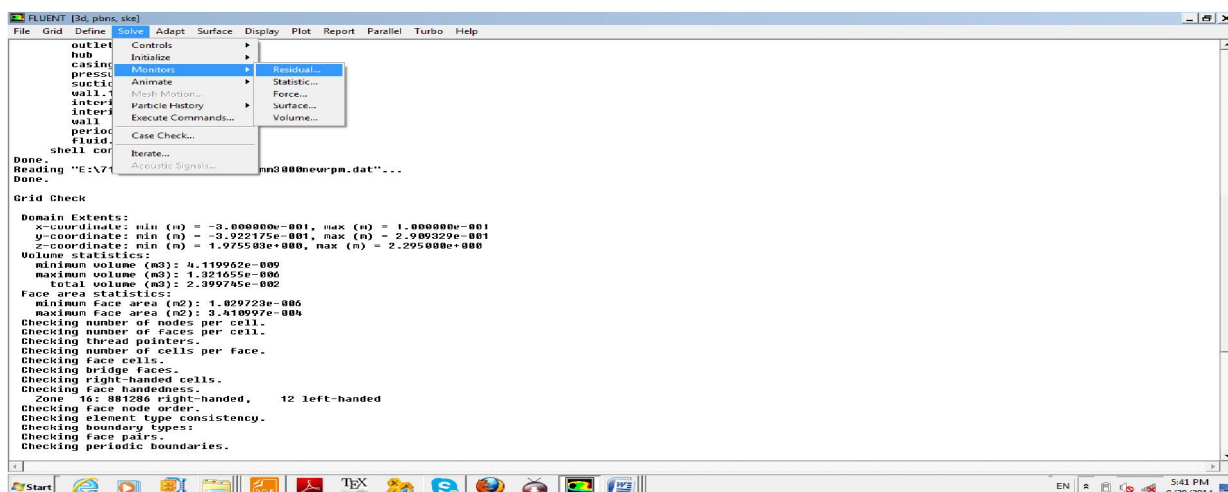
2- Enable the plotting of residual during the calculation.

Diagram illustrating the workflow:

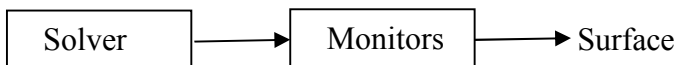
```

    graph LR
        Solver[Solver] --> Monitors[Monitors]
        Monitors --> Residual[Residual]
    
```

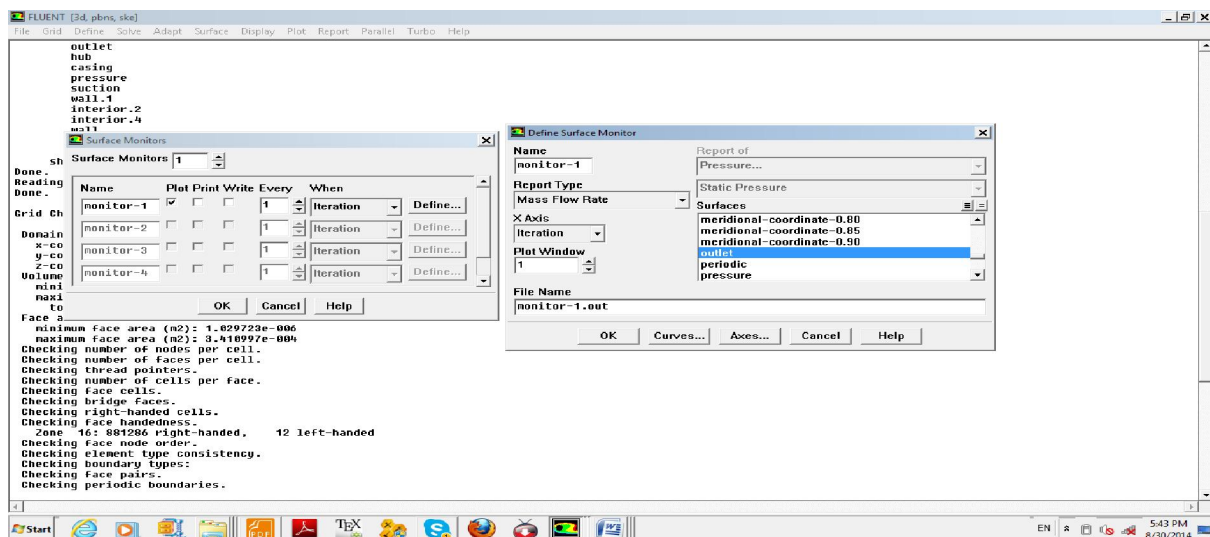
- Under Option select plot.
- Click OK .



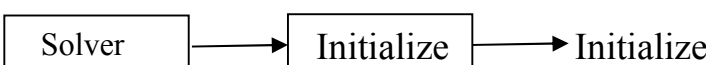
### 3. Enable the plotting of mass flow rate at the outlet.



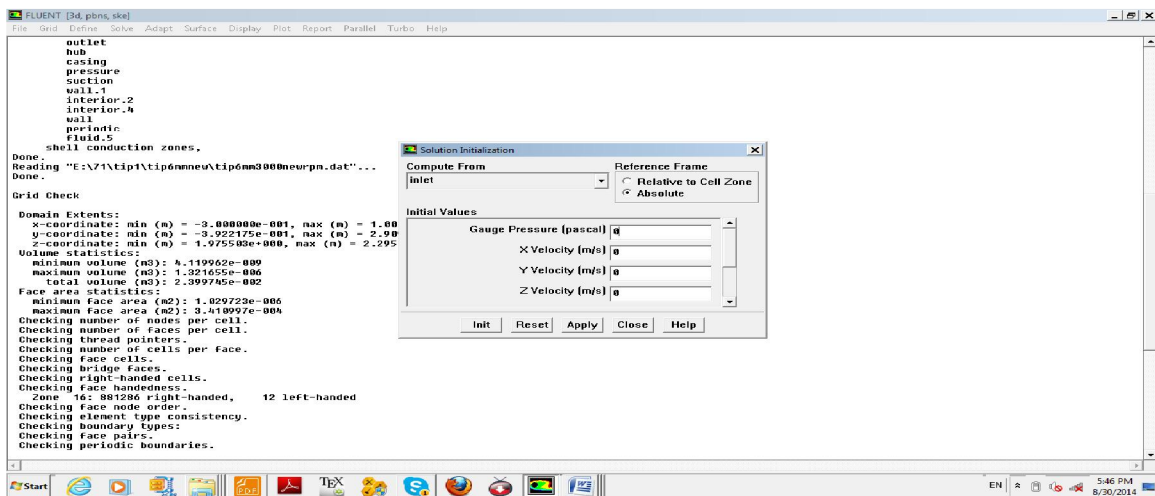
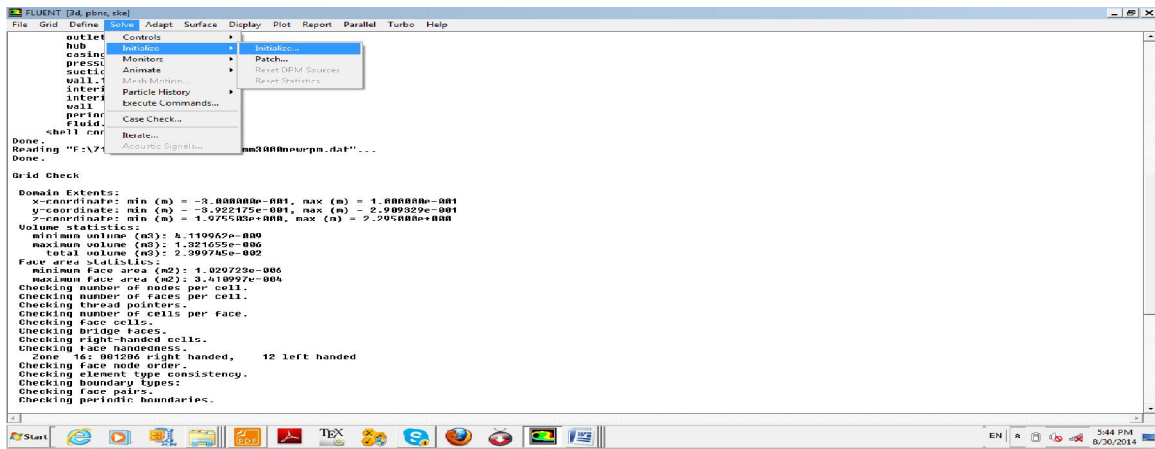
- Increase NO of plot to 1.
- Turn on the plot and write(Note )option for monitor .
- Click on Define to specify the surface monitor parameter in define surface monitor.
  - select mass flow rate from the report type drop-down list.
  - select outlet in the surface .
  - Click on OK to define the monitor.
- Click on OK in the surface monitor panel to enable the monitor.



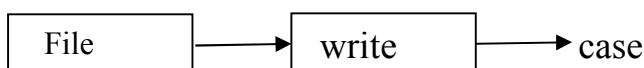
### 4. Initialize the flow field.



- Select pressure-inlet in the Compute From drop-down list.
- Click Init, and Close the panel.

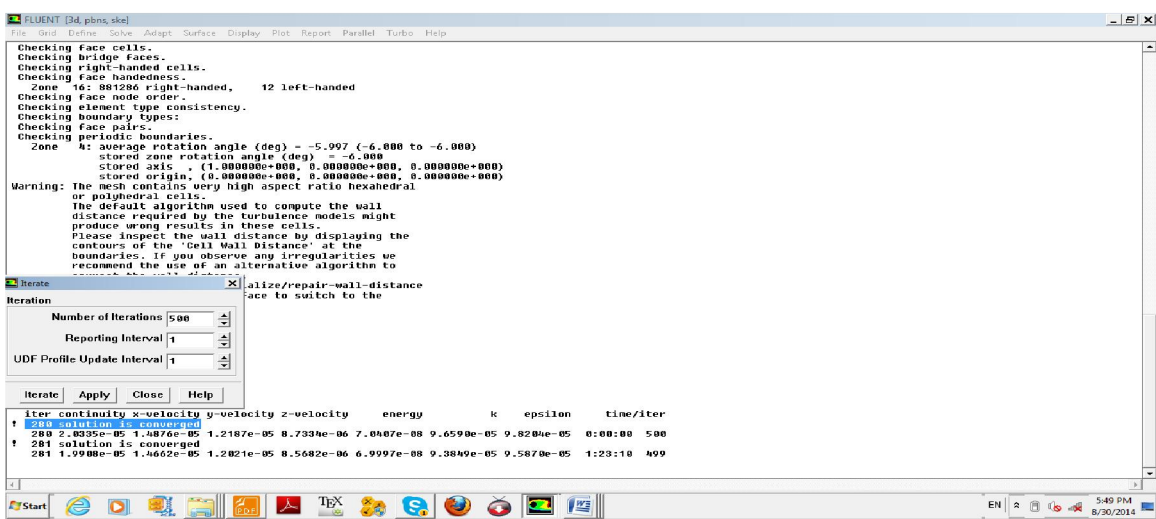
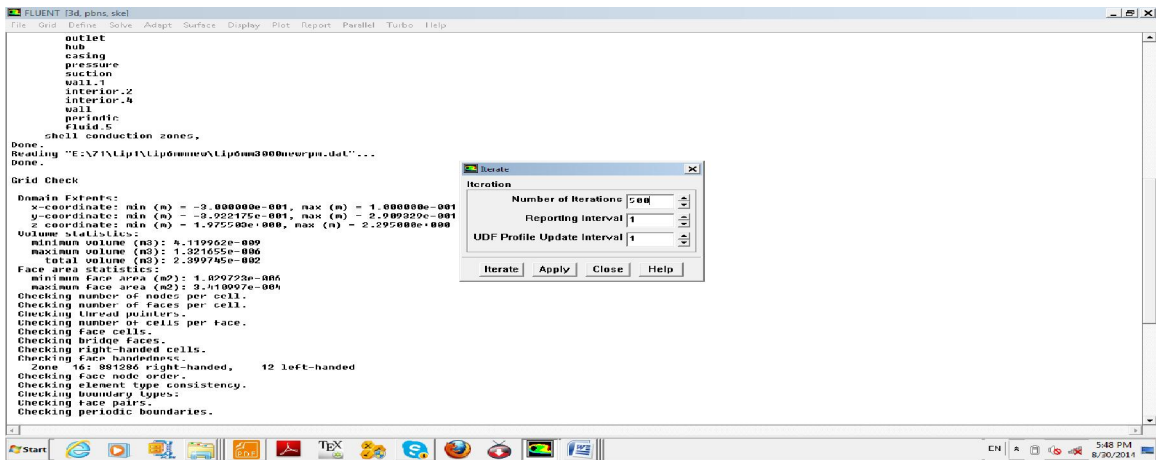


## 5. Save the steady flow case file (name.case)



## 6. Start the calculation by requesting 500 iterations.





!calculation until the mass flow rate at outlet to be constant .